ON -LINE MONITORING OF TOOL WEAR AND CONTROL OF DIMENSIONAL INACCURACY IN TURNING

A Thesis Submitted
in Partial Fulfillment of the Requirements
for the Degree of

MASTER OF TECHNOLOGY

By

N.SHIVA RAMA KRISHNA

to the

DEPARTMENT OF MECHANICAL ENGINEERING
INDIAN INSTITUTE OF TECHNOLOGY KANPUR

August 1998

CERTIFICATE

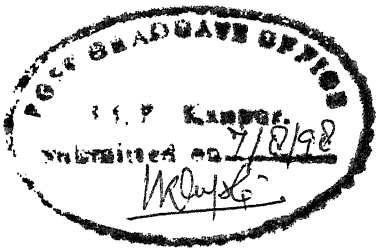

It is certified that the work contained in the thesis entitled " ON-LINE MONITORING OF TOOL WEAR AND CONTROL OF DIMENSIONAL INACCURACY IN TURNING " by Mr.N.Shiva Rama Krishna , has been carried out under our supervision and this work has not been submitted elsewhere for a degree.

Dr. S. K. Choudhary
Associate Professor,
Dept. of Mechanical Engg.
IIT Kanpur.

Dr. V. K. Jain
Professor,
Dept. of Mechanical Eng
IIT Kanpur.

DEDICATED TO MY BELOVED PARENTS WHO SACRIFICED THEIR TODAY FOR MY BETTER TOMORROW.

Acknowledgment

I would like to express my deep felt gratitude and appreciation to my thesis supervisors Dr. S.K.Choudhury and Dr. V. K. Jain for their skillful guidance, constant supervision, timely suggestions, constructive criticisms in completing of this project within the stipulated time.

I am thankful to all the students of the manufacturing science stream for maintaining lively atmosphere with discussions. My special thanks to K. M. Ramesh , T. Rajani Kumar for their help in the preparation of final experimental setup and in the writing up of the thesis report.

I would also like to thank my friends K.Siva Prasad, Venkata Ramana, G. Prakas Sastry, M. Anil Kumar, Arvind Shukla, I. V. Rao, C. Srinivas Rao, and k. Easwar Kumar for their consistent inspiration for completion of the project.

Many special thanks to Mr. R.M.Jha, Mr. H.P.Sharma, Mr. Namdeo, Mr. Deepak and Ms Anjali Kulkarni for their help during experimentation. Their experience and expertise has been of great help in solving the practical problems encountered.

Finally, I express thanks to all my friends, who made my stay here a memorable and enjoyable one.

Contents

List of Figures

List of Tables

Nomenclature

v	:	Cutting velocity
f	:	Feed rate
d	:	Depth of cut
h_f	:	The flank wear land
x_i	:	Input cutting parameters
z_i	:	i^{th} component of the output pattern
y_j	:	Actual response of the j^{th} neuron
d_j	:	Desired response at the j^{th} output neuron
e_j	:	Error at the j^{th} neuron
E	:	Sum of squared errors over the input neurons
v_j	:	The net internal activity of the j^{th} neuron
α	:	Momentum constant
η	:	Learning rate constant
δ_j	:	Local gradient at j^{th} neuron
$\phi(x)$	:	The activation function
a, b	:	Constants in the hyperbolic tangent function
$w_{ji}(n)$	:	Weight of the connection between the j^{th} neuron and the i^{th} neuron in the previous layer for the n^{th} iteration
Δw_{ji}	:	Change in the weight of the connection between the j^{th} neuron and the i^{th} neuron in the previous layer for n^{th} iteration

θ_c : angle of incidence on the optical fibre

Abstract

Metal cutting is one of the most important and vital machining processes among all the manufacturing processes. In metal cutting excess metal is removed in the form of chips to form the desired shape using a wedge shaped tool. Turning is a metal cutting process where the single-point cutting tool is used to remove the excess metal from the workpiece. There are various problems that generally effect the dimensions of the workpiece during machining. Among them tool wear is the most significant one. Tool wear causes a tapered surface instead of a cylindrical one especially in turning of long jobs. The present work is dedicated to develop a sensor which monitors the tool wear and controls the workpiece diameter so as to avoid the tapering in the machined job.

A non contact, displacement optical fiber sensor is developed to monitor the tool wear indirectly by constantly monitoring the change in the workpiece diameterdue to the tool wear. The signal from this optical fiber sensor, is amplified and converted into digital form. This digital signal is sent as an input to the system(software) developed where it is compared with the previously stored signal to estimate the change in the workpiece diameter, and hence the tool wear. This difference corresponds to the radial tool wear, which is then sent as an input to the trained neural network module for predicting the flank wear and also to the controlling module to control the dimensional inaccuracy of the workpiece due to the tool wear. The flank wear data with different working conditions were collected experimentally to train the neural network for predicting the flank wear. The sensor was tested for different working conditions. Whenever the controlling module is invoked, it sends the required amount of signals to a stepper motor through a PC interfacing circuit to compensate the dimensional inaccuracy due to the tool wear. The results show that dimensional inaccuracy can be maintained below 0.03 mm using the developed system.

Q:- What is tool wear ?

A:- What are various things that are tool wear, that affect the dimensions of work-piece during machining

Chapter 1

Introduction

The major goal of manufacturing systems is to integrate the machine tools which have the intelligence to look after themselves and their peripheral devices. Due to increased competition in the market, need of high quality products with less cost, and requirement of high productivity, there is a high demand of automated systems. In the world of conventional manufacturing, metal cutting is an area where the wedge shaped tool is used to get the required shape and size of the workpiece. But due to various technological problems it is becoming very difficult to make this process fully automated. For example, the tool is used for cutting the workpiece materials; the tool in turn wears out, continuously or intermittently. Due to this tool wear there are some side effects which are listed below.

- Increase in machine tool vibration,
- Increase in dimensional instability of the work piece,
- Change in cutting conditions,
- Effect on surface finish of the job produced, and
- Increase in the cutting forces.

A cutting tool is said to be failed if it produces the dimensional deviations more than the required limits and unacceptable surface properties. A cutting tool is the only one component that wears very rapidly in the machine tool and needs to be minimized.

The present work is dedicated to monitor the tool wear and solve the dimensional instability side effect.

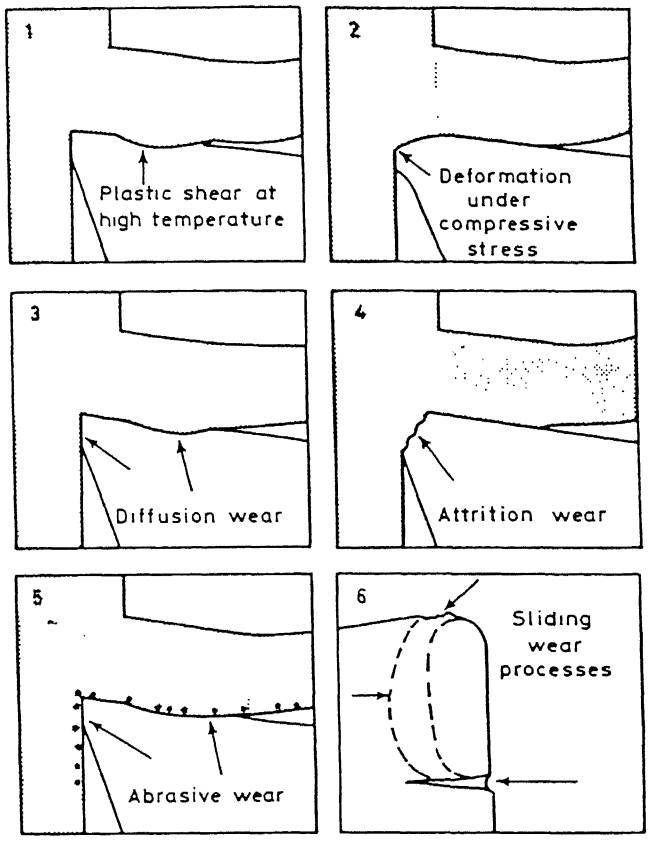

Figure 1.1: Different types of Tool Wear.[1]

1.1 Tool Wear in Metal Cutting

Although the exact form of tool wear will vary according to the cutting operation, that is turning, milling, drilling etc., the study of tool used in turning which is a single point cutting tool will give an overall idea.

There are various types of wears as shown in the Fig. 1.1. The reason for the occurrence of a particular type of wear or their combination depends upon the cutting conditions, materials of the workpiece and the tool used. Figure 1.1 shows different types of tool wear in a typical HSS tool.[1]

The reasons for the various tool wears are given as below.

1.1.1 Plastic deformation by shear at high temperature

At high temperatures the tool hardness will decrease and as the worn material flows above the tool it will deform the tool material. This type of wear is called crater

wear. This is generally formed at certain distance from the cutting edge because the higher temperatures will be developed at certain distance from the cutting edge. Crater wear is formed when cutting speed is high.

1.1.2 Deformation under compressive stress

In this case the material is not removed, rather deformed, but forces and temperature may be increased locally and so the flow pattern of the workpiece will be modified. Tools are more likely to be damaged by deformation when the hardness of the work material is high and it is this mechanism that limits the workpiece hardness that can be machined.

1.1.3 Diffusion wear

There is metal to metal contact and temperature of 700^o C to 900^{o}C are high enough for appreciable diffusion to take place. Thus tools may be worn by metal carbon atoms from the tool diffusing into, and being carried away by the stream of work material flowing over its surface, and by the atoms of the work material diffusing into or reacting with the surface layers of the tool to alter and weaken the surface. Rates of diffusion increase rapidly with temperature.

1.1.4 Attrition wear

The flow of metal past the cutting edge is more irregular and less stream-lined or laminar. In this case a built-up edge may be formed on the tool. Under these conditions microscopic size of materials may be torn intermittently from the tool surface, and this mechanism is called attrition.

1.1.5 Abrasive wear

Abrasion is considered as a major source of wear and literature on the subject often describes tool wear in general as abrasive. Work material contains greater concentration of hard particles, such as pockets of sand on the surface of casting causing rapid abrasive wear of the tool material.

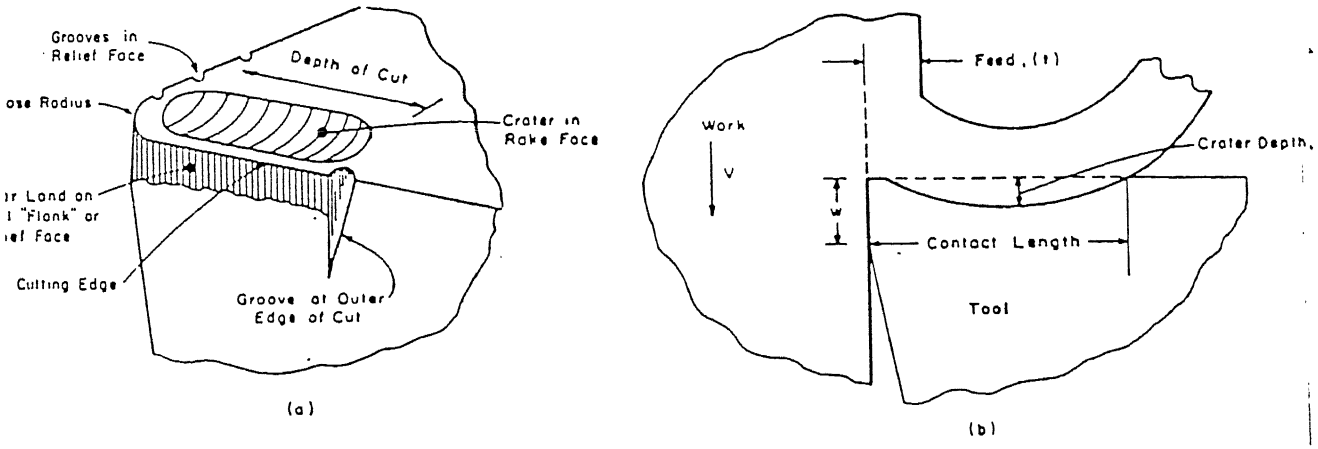

Figure 1.2: Tool Wear nomenclature [2]

1.1.6 Wear under sliding conditions

This type of wear takes place when sliding occurs, either continuously or intermittently, other wear mechanisms can come into play and, under suitable conditions can cause accelerated wear in these regions.

There are other wear mechanisms that are still under investigations. However wear results in distortion of some specific areas of the cutting tool. Figure 1.2 shows the geometry of the worn tool and its nomenclature.

The flank wear is more important to study as compared to all other types because it governs the dimensional accuracy and surface finish of the machined component. It also influences the chatter of the machine tool. Most of the research works reported in the literature are related to the flank wear. The following paragraphs will give the need of the on-line monitoring and on -line control of dimensional inaccuracies on the machined components.

1.2 On-Line monitoring of tool wear

Use of a worn-out tool during cutting may damage the workpiece to the highest extent. Further the tool failure depends on multiple of factors, so it is difficult to predict when the tool will cross pre-specified limit. Therefore there is a need of sensor that

The sensors which can be used to monitor tool wear during cutting should have the combination of the following characteristics.

- It must give fast ,clear and reliable signal.
- It must be practical and able to work without any operational difficulties on the shop floor.
- It should be flexible and able to monitor and control tool at all working conditions.
- It must be capable of monitoring the tool wear On-Line to minimize the production time.
- It should permit remote monitoring and should not interfere with machining process.
- It should be cheap, safe and reliable under varying working conditions like temperature, pressure etc.

1.3 On-line control of Dimensional deviations

The tool wear is inevitable. One of the major problems caused by it is, dimensional instability. The tool wear in radial direction occurs mainly at medium cutting speeds and high feeds. Figure 1.3 shows how the tool wear effects the dimensions at macro level of the job to be produced in turning .The dimensional deviations in turning can also be due to

- The machine inaccuracy.
- The machine tool vibrations

However if the above factors are under control then the tool wear will be the dominating factor responsible for dimensional deviation.

The dimensional deviations will affect the production cost due to the increased production time because of increase in the amount of material to be removed during finishing operation. Figure 1.3 shows the extra volume of the job to be removed due to the taper produced in the workpiece because of flank wear of the tool.

$$\text{Extra volume} = \Pi\ D_f \text{ x l } (D_f \text{ - } D_i)$$

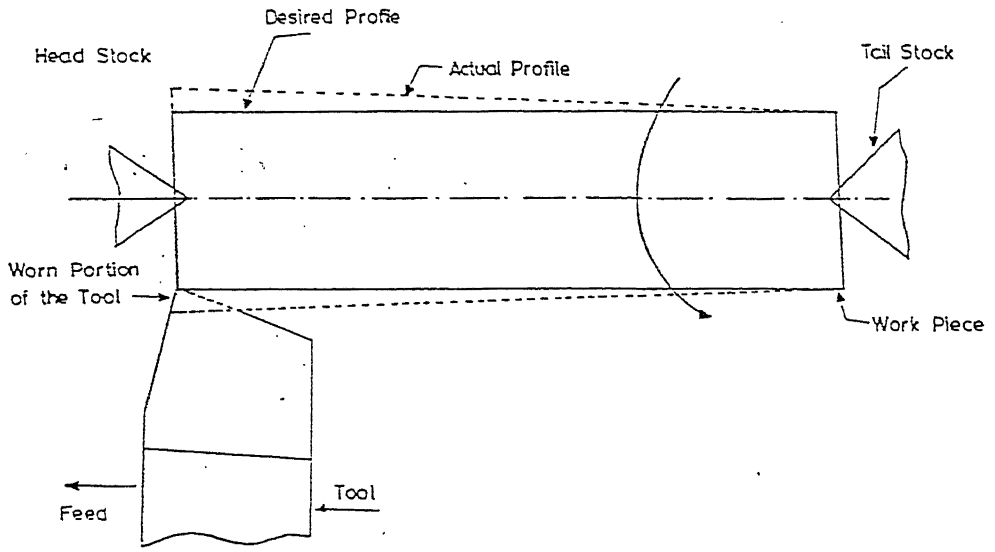

Figure 1.3: Diagram Showing the Effect of tool wear on Dimensional Accuracy

where

- D_f = Final diameter ,D_i = Initial diameter
- l = Length of the Job to be produced

For long workpiece like turning of a gun barrel even a small change in the diameter will cause the large increase in extra volume. As the volume of the material to be removed increases the grinding cost and the time increase, increasing ultimately the production cost and production time.

This problem needs a solution. The solution can be of two types. One is to restrict the tool wear and another is to compensate the dimensional deviations on-line by developing a reliable sensor.

1.4 Literature Review

A lot of research work has been done over the last 40 years in the area of metal cutting for developing the sensors which can give a reliable information about the tool wear. Some theoretical models and a variety of techniques, supplemented with experiments, were proposed for on-line monitoring of tool wear during machining.

Various techniques proposed for monitoring the tool wear are generally classified into two broad categories : Direct and Indirect methods.[3] Table 1.1 shows the classification of these methods. In indirect methods, a suitable parameter is selected to provide information about the tool state, while in direct methods the actual wear on the tool is measured. The inherent advantage of the indirect techniques is that they can be used without actually interrupting the cutting process.

Anuj Sanjanwala [4] developed a pneumatic sensor for on-line measurement of the workpiece dimensions change during turning. A compressor is used as source of the compressed air .The compressor surge tank has two openings. One is connected to the pneumatic sensor and the other is connected to the man port of the pilot controlled direction control valve. The air coming to the pneumatic sensor first passes through an orifice and then through a nozzle. The pressure between the orifice and the nozzle, called back pressure, depends upon the distance between the nozzle and workpiece which decreases as the workpiece diameter increases with the tool wear.

Shirashi and Uehara[5] developed a non-contact measuring apparatus. They used this apparatus for in-process control of NC lathe. The proposed apparatus was realized by the use of a laser unit, photo conductive cells and optical systems. The finished size of a workpiece was continuously monitored by the laser spot and the tool post was automatically controlled to reduce the error.

Suzuki and Weinmann[6] devised an on-line tool wear sensor by measuring the change in distance between the tool holder and workpiece using stylus which is mounted on a tool holder. The stylus movement is sensed by a displacement traducer. The tool wear was monitored using a digital processing oscilloscope.

K.C.Fan and Y.H.Chao[7] developed a set-up for in-process dimensional control of the workpiece during turning. During operation ,the diameter of the workpiece can be measured through three servo measurement units. Each unit is composed of a non - contact proximitor for direct gap sensing, a stepping motor controlled a linear carriage to move the proximeter for surface tracing, and a LVDT for position feedback of the carriage. The error compensation strategy is implemented by interrupting a compensator in the position feedback loop of the NC servo system so that the tool position can be directly controlled by an external personal computer.

M.Shiraishi and S.Sato [8] developed system for dimensional and surface roughness

Table 1.1: Classification of Tool Wear Sensing Methods. [3]

Procedure	Measurement	Transducer
DIRECT		
Optical	Shape or position of the cutting edge	TV camera; optical transducer
Wear particles and radioactivity	Particle size and concentration; radioactivity	Spectrophotometer and the Scintillator
Tool-work junction resistance	Changes of the junction resistance	Voltmeter
Workpiece size	Dimension of workpiece	Micrometer; optical, pneumatic, ultrasonic electromagnetic transducers
Tool-work distance	Distance of work-tool from tool holder	Micrometer; pneumatic guage; displacement transducer
INDIRECT		
Cutting force	Changes of cutting force	Dynamometer strain guage
Acoustic emission	Stress wave energy	*AE* transducer
Sound	Acoustic waves	Microphone
Vibration	Vibrations of tools and/or tool posts	Accelerometer
Temperature	Variation of cutting tool temperature	Thermocouple; pyrometer
Power input	Power or current consumption of spindle or feed motor	Ampere meter; dynamometer
Roughness of machined surface	Changes in surface roughness of workpiece	Mechanical stylus; optical transducer

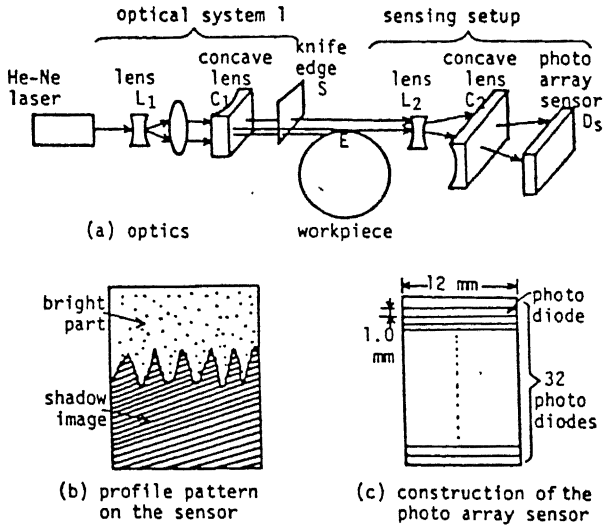

Figure 1.4: Measuring System. [8]

controlling in turning operation. The measuring principle is as shown in the Fig. 1.4. A He-Ne laser light, having a rectangular beam by traversing lens (L1) and corresponding light after passing over the workpiece profile is sensed by 32 photo diodes. Each photo diode can provide an output signal. The signals are processed and corresponding profile was measured.

An optical fiber sensor based on cutting force measuring device was developed by the W.L.Jin, P.K.Venuvinod and X.Wang[9].In this system a specially made tool sank attached with optical fiber sensor was developed. The tool sank was treated in such a way that during a cutting process a displacement proportional to cutting force.

The workpiece diameter change can also be measured using the ultrasonic sensors .This technique was given by G.f.Micheletti ,W.Koneing and H.R.victor [10].

1.5 Objectives and Scope of Present Work

The research was done for both on-line and off-line sensing of the tool wear. Conventionally, the tool wear is measured by removing it from the tool post and placing the same under the microscope. Off -line sensors can save this wastage of production time. Most of the on-line sensors developed were based upon indirect measuring techniques which are not suitable to all conditions.

The present work involves development of a sensor for on-line sensing and control

of dimensional deviations occurred due to tool wear in turning operation. A fiber optic sensor is used for predicting the flank wear with this dimensional change for various cutting conditions like cutting speed ,feed and depth of cut on center lathe. The control system will act according to the tool wear signal obtained from the sensor system. The objectives of present work are

- Design and fabrication of a device to sense tool wear during machining of workpiece.
- Design and fabrication of an actuator to arrange stepper motor and worm gears which controls the tool post according the tool wear.
- Design and fabrication of a feed back control system components(PC interfacing circuit) that connect the sensing and compensating components.
- Design and development of an user friendly and menu driven software for on-line tool wear monitoring, predicting flank wear using neural network technique and operating the controlling system which maintains the dimensional deviations under control.
- Assembly of the system components.
- Testing of the designed and fabricated system by conducting the experiments which are designed by following the statistical methods.

1.6 Organization of Thesis

The thesis is organized in various chapters. Chapter 2 gives the information about the experimental set-up ,which involves optical sensor system and the controlling system and its various parts . This chapter idea about the PC interfacing and controlling the hardware.

In chapter 3, the software written for sensing ,controlling and predicting the tool wear, which has been written in the form of various modules has been discussed in depth. For predicting the tool wear, **Neural networks** has been used. This chapter also gives details of the Neural networks used and the derivation of the **Back propagation algorithm.**

In chapter 4, the experiments conducted to test the performance and efficacy of the sensor designed to control the dimensional deviations in turning, and various measures taken to conduct the experiments have been discussed. Finally the limitations of the sensor designed are also discussed.

In chapter 5 ,conclusions of the thesis work have been drawn and scope for future work has been elaborated.

Chapter 2

EXPERIMENTAL SET-UP

The wear due to interaction between the chip and tool, and between the work and tool are the main phenomena by which a cutting tool fails. Out of various tool wear phenomena the radial tool wear causes the undesired dimensional instability. There are various other reasons for dimensional instability other than tool wear which were discussed in the previous chapter. This chapter deals with the design and fabrication of the optical sensor, which measures the change in diameter of the workpiece due to the radial tool wear. This chapter also discusses the development of a control system for the tool post to compensate the tool wear in radial direction. The personal computer has been used to work as a logical unit to control the position of the tool according to the signal obtained from the optical sensor. For communication with the hardware set-up interfacing circuits were designed.
The full details are presented in the later sections.

2.1 OPTICAL SENSOR

A sensor is a device that converts the change in magnitude of one physical parameter into a corresponding change in another parameter that can be measured conveniently and accurately.

Fiber optic sensors have proved to be accurate and capable of operating in harsh environments contaminated with high explosives or corrosive gases. Some of the key features of fiber optic sensors compared to conventional ones are

- increased sensitivity.

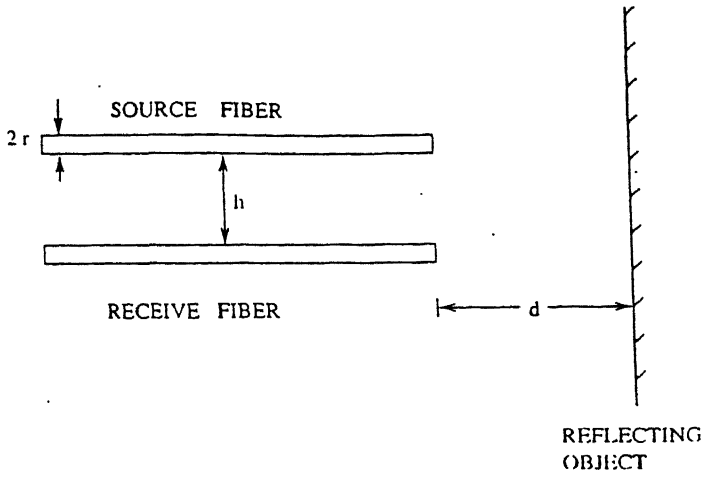

Figure 2.1: Basic Reflective Fiber Optic Sensor [11]

- Geometric versatility i.e. fiber sensor can be configured in arbitrary shapes.
- highly reliable and safe.
- very compact.
- access to normally inaccessible areas.

The schematic diagram of a basic Fiber optic sensor is shown in the figure 2.1

The reflective intensity modulated fiber optic sensor is one of the simplest and the most widely used sensor. It can be used as a displacement sensor in vibration and monitoring sensor in robotics and automation control. In the present work, this type of sensor has been used to measure a change in the workpiece diameter.

The basic operating principle can be explained by considering the transmissive system where an image of the emitting fiber is formed at a distance d, behind the reflective surface. This is as shown in the figure 2.2

The light is emitted from the image fiber in the shape of a cone. Depending on distances from the receiving fiber and the reflector(d) and between the emitting and receiving fibers(h), the receiving fiber can be

- Out of light cone,
- Partially overlapped by the emitted cone,
- Fully overlapped by the emitted cone.

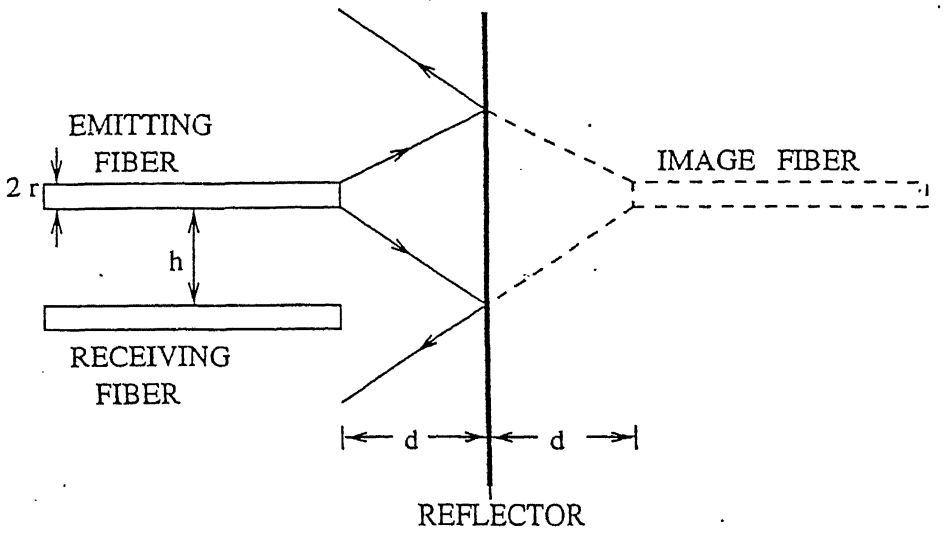

Figure 2.2: Reflective Fiber with image Fiber. [11]

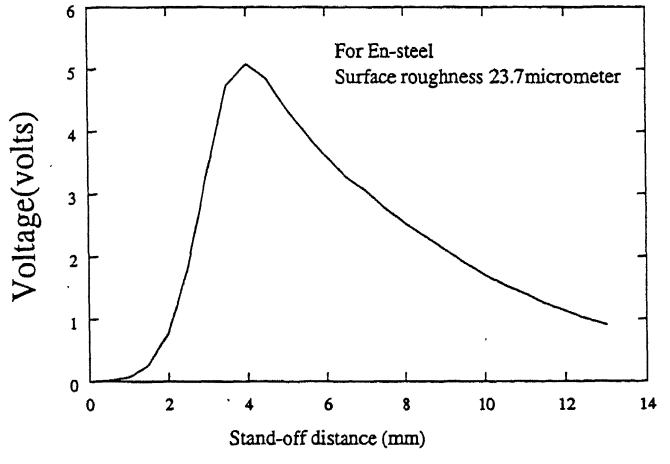

Figure 2.3: Chareterstic curve of the sensor

When the distance d (stand off distance) is zero then the light emitted from the emitting fiber is returned back and thus the voltage obtained which is direct measure of the intensity of the light coming from the receiving fibers is also zero. In this case the receiving fibers are out of the cone .

As the d increases the cone of light partially overlaps with the receiving fibers and the voltage increases linearly. The slope for this region is very high and is also named as **Front slope.**

At certain distance 'd' the cone fully covers the receiving fibers and the voltage at this stage is maximum. After this limit, if d increases further then the light intensity will decrease as the cross sectional area of the cone at the receiving fibers increases. Due to this reason the voltage will also decrease. The slope for this region is negative and named as **Back slope.** The curve in the figure 2.3 shows the front slope and back slope. This curve is called as *chareterstic curve.* This curve is drawn by conducting the experiments. In that curve the light intensity is represented as voltage. In the present work the front slope has been selected due to the high sensitivity of sensor in this region. Generally the back slope is used for large range of operations and front slope is for high sensitive operations.

2.1.1 Optical Fiber Transducer

Most of the fiber optic transducers basically use some form of the optical lever principle (a means of detecting small displacements by reflected beam of light from the object). Fig.2.4 shows the cross-section of a step index multi-media fiber [12]. These fibers are made of a cylindrical core, typically 50 micrometers in diameter, surrounded by a cladding whose refractive index is less than that of the core. The numerical aperture of the fiber in air is given as :

$$NA = sin\theta_c = \sqrt{n_1^2 - n_2^2} \tag{2.1}$$

where n_1 and n_2 are the refractive indices of the core and the cladding material, respectively and θ_c is the angle of incidence of the ray incident at the core-cladding interface at the critical angle for total internal reflection. This ray consequently propagates along the fiber with no reflection losses.

Usually the sensor consists of a bifurcated fiber bundle with one leg connected to a photo detector and the other to a light source (preferably monochromatic). At the face of merger of the two bundles the fibers from the two legs are randomly mixed. Other configurations with hemispherical or concentric- traverse-inside fiber grouping are also

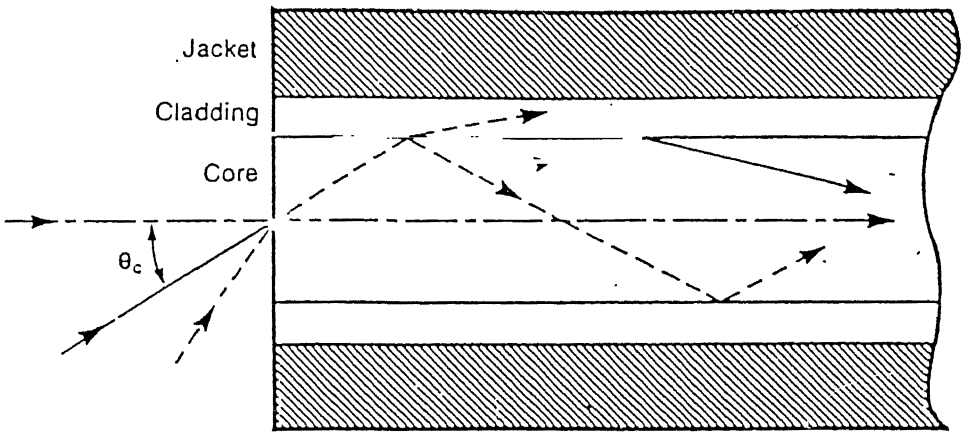

Figure 2.4: Ray propagation through a multi-mode optical fiber [12]

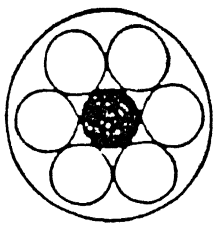

Figure 2.5: The cross section of the bundle of fibers used in the present work

available.

For the experiments conducted in this work, a bifurcated bundle of optical fibers, with concentric traverse inside (CTI) grouping of the fibers at the merger point, was selected.

The overall arrangement of the optical fiber sensor is as shown in the figure 2.6.

2.2 Sensing and Amplification Circuit

The light is reflected from the surface of the workpiece when it is incident on it by the center core of fiber optic transducer and this will be received by the receiving fibers. The power of the reflected light is dependent on the workpiece dimensions(diameter). This reflected light energy is converted in electrical signal using photo detector. Photo detection involves measuring the incident light in terms of an electrical signal. There are

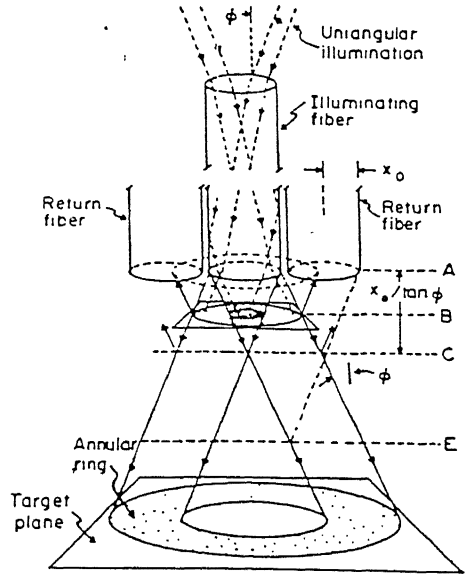

Figure 2.6: Operating principle of the designed optical fiber

three basic forms of photo detection. They are

- Photo emission.
- Photo conduction.
- Photo voltaic.

photo emission means when the light rays fall on the detector surface then free electrons will be emitted. This emission usually occurs in a vacuum tube.

With *photo conduction* the incident light on a photosensitive material causes the photo detector to alter its conductance.

In the *photovoltaic* action, a voltage is generated when the light strikes the sensitive material in the photo detector.

The commonly used photo detector is the single junction photo diode. A photo diode is the optical version of the standard diode. It is constructed of a $P-N$ junction. Photons of light energy are absorbed into the device and the hole-electron pairs are generated. The pairs are combined at different depths within the diode depending on the energy level of the photon. A wide, thin surface area is used to ensure maximum absorption. Current flow is dependent on the amount of radiation absorbed. Photo diodes operate in the photo conductive mode with reverse DC bias applied. This is also known as the current mode. Current is extracted as a measure of the applied radiant energy. Signal current

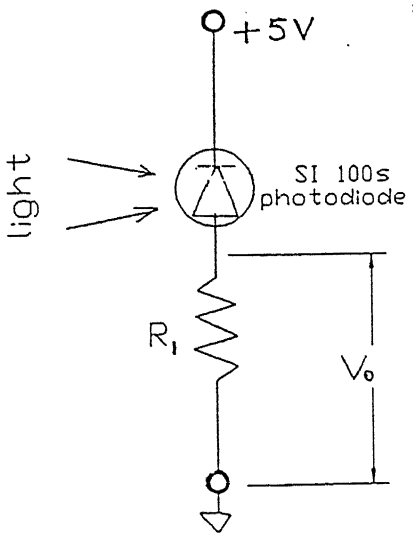

Figure 2.7: Photo diode circuit

flows through the load resistor, R_1, in the photo conductive circuit, as shown in Fig. 2.7.

The detecting material should be such that whenever it is exposed to light it should absorb the light energy. If the detector responds to the light energy and not the wavelength, it is said to be non-selective. If the detector responds by varying detection at different wavelengths, it is known as selective. Selectivity or responsivity is the detector's response per unit of light. Wavelength responsivity is called the spectral response. Frequency response is the speed by which the detector responds to the changes in the radiation amplitude. Fluctuations in the output current and/or voltage are referred to as noise. Noise is usually caused by current that flows in the detector regardless of whether light is applied or not. A common specification for the detector is the signal-to-noise ratio which is a ratio of the signal current divided by the noise current.

In the present work, a SI 100s photo diode with a responsivity of 0.4 A/W at 632.8nm wavelength is used. The specifications are shown in the Appendix I.

The voltage available after the photo detection is few milli volts. To have more sensitivity the signal is amplified and for this purpose a pre-amplification circuit is designed. The amplifier is used with commercially available Op-amp IC. The circuit is shown in the Fig. 2.8.

The difference in the voltage signals at the two inputs is amplified by an operational amplifier which can operate either in inverting or non-inverting mode. The voltage will be developed across the load resistor(R_1) of the photo diode whenever any light incidents upon it. This is fed as one input to the op-amp, the other input is grounded with another resistor, R_2, R_3 is the feedback resistor. The required gain factor is obtained by changing values of the two resistors, R_3 and R_2. Initially with the two inputs of the op-amp shorted and grounded, the output voltage is set to zero using the variable resistor, R_4.

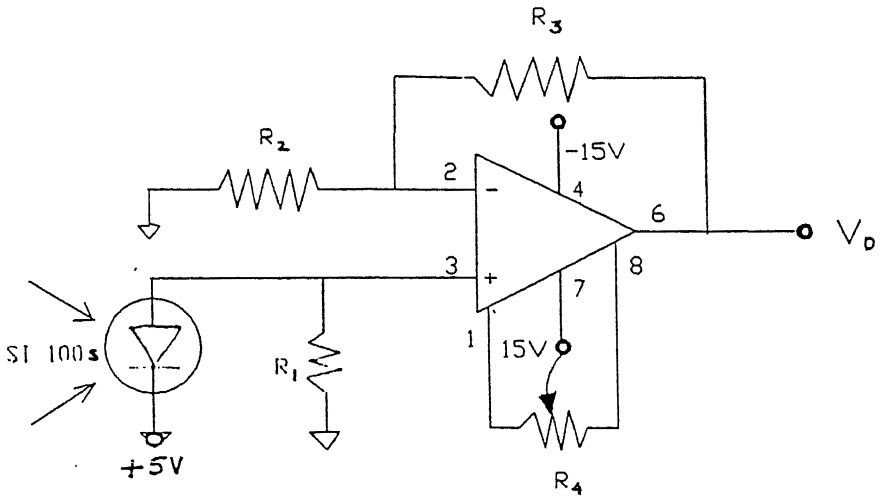

Figure 2.8: The sensing and amplification circuit

The method of doing for zero voltage output when the op-amp is short circuited is called input offset voltage correction. This correction is done carefully before using the circuit for the operation, otherwise the op-amp will be driven into a *saturation region* giving a constant output voltage for any input voltage signal. The gain used in the present work is calculated as follows:

$$G = \frac{R_3}{R_2} \tag{2.2}$$

The output voltage is found as

$$\begin{aligned} V_o &= (1 + \frac{R_3}{R_2})\,(I_p R_1) \\ &= \zeta(1 + \frac{R_3}{R_2}) P\, R_1 \end{aligned} \tag{2.3}$$

where, ζ is the responsivity of the photo diode and P is the wattage of the light incident on the photo diode.

In the present work the Laser is used as source of light. The following section will give the reason for using laser as the source of light.

2.2.1 LASERS

The name LASER is an acronym of light amplification by stimulated emission of radiation. A LASER is a device that produces an intense concentrated, and highly parallel beam

of coherent light. In present work the He-Ne laser was used as light source though other light sources can serve this purpose but laser can do it in efficient way and the efficacy will be more due to the following special properties.

- Coherence
- Divergence
- High concentrated power

2.2.2 Coherence

Coherence probably is the best known property of laser light . Light waves are coherent if they are in phase with each other, that is if their peaks and valleys are lined up at the same point.

2.2.3 Divergence

The divergence of the Laser light is very less compared with other sources of light . Due to this reason it is used to measure the astronomical distances. In the present work the laser light is used basically due to its less divergence angle and negligible loss of power.

With the above said special properties the LASER will have more reflecting light power resulting in high sensitivity for the sensor developed. The Fig. 2.9 shows the comparison between the output when light source is used and when a halogen light source is used for a typical optical fiber sensor. [11]

2.3 Analog to Digital Conversion

The signal obtained from the sensing and amplification circuit is of the analog form. Here the logic unit used for giving the control signal when ever desired and for predicting the tool wear is a PC. To give this signal to the system developed (details are discussed in the next chapter) ,it should be converted into the **Digital signal.** Among the various techniques available for A/D conversion, Successive Approximation Method is the most popular method. In this technique, various output codes are fed into a D/A converter and the result is compared with the analog input by a comparator, as shown in the Fig. 2.10. The way it is usually done is to set all bits initially to zero, and beginning with the

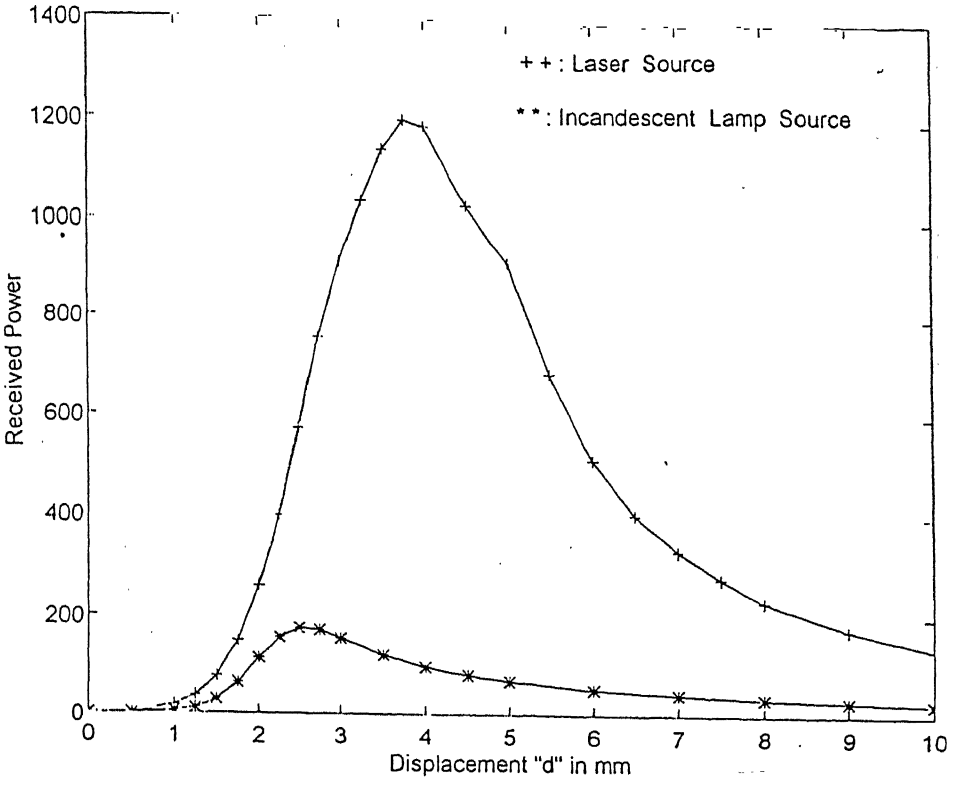

Figure 2.9: The Comparison of the output with Laser and Halogen light source. [11]

most significant bit, each bit in turn is set to one. If the D/A output does not exceed the analog input signal voltage, the bit is left as a one, otherwise it is set back to zero. For an $n - bitA/D$, n such steps are required.

A successive approximation A/D module has a BEGIN OF CONVERSION input and END OF CONVERSION output. The digital output is always provided in the parallel format. Successive approximation A/D converters are relatively accurate and fast, requiring only 'n' settling times of the DAC for $n - bit$ precision. This type of converter operates on a brief sample of the input voltage and if the input voltage is changing during the conversion, the error is not greater than the change during that time.

A commercially available data acquisition card for $IBMPC/XT/AT$ computers, $PCL-812$ from Dynalog Microsystems Ltd., is used in the present work. This uses an industrial standard 12-bit successive approximation converter $ADC574$ to convert the analog inputs. The specifications and features of this card are shown in Appendix 1.

The A/D conversion is triggered using a software which is discussed fully in the next chapter , controlled by the application program issued software command. The data transfer is also done using the program control. After the A/D converter has been trig-

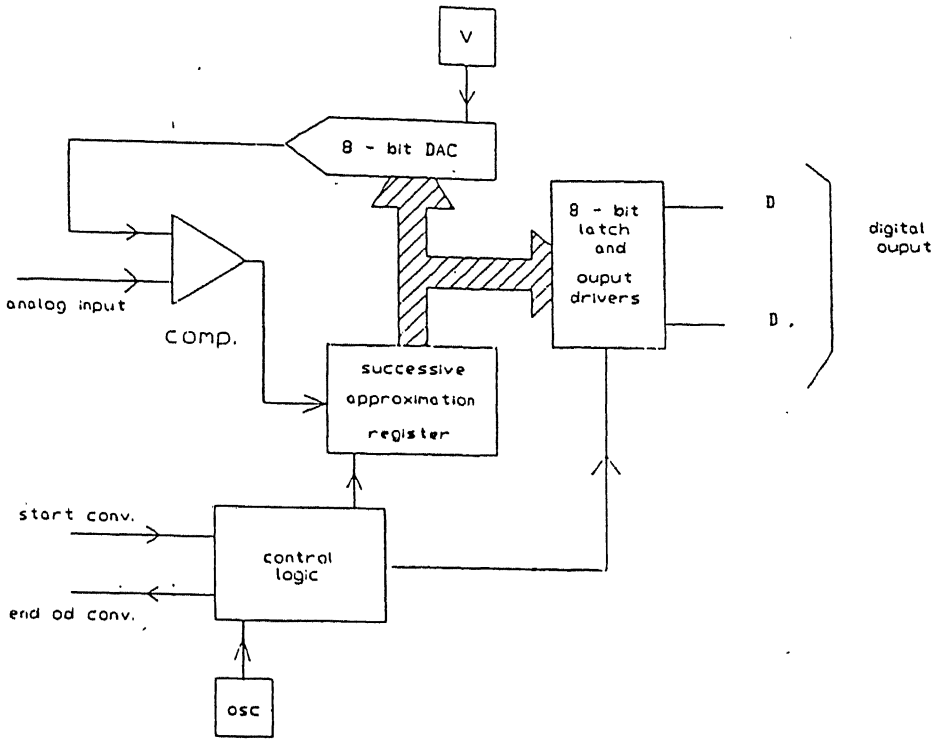

Figure 2.10: Successive approximation ADC. [13]

gered, the application program checks the END OF CONVERSION (*EOC*) bit of the *A/D* status register. If the EOC is detected, the converted data is transferred from the *A/D* data register to computer memory by the application program control. The next chapter gives the algorithm for analog to digital conversion.

2.4 Actuator

After receiving compensating signal from the PC there is a need of actuator for compensation of the workpiece dimensions change. The Actuator will serve that purpose. Fig. 2.11 shows the line diagram of the actuator.

The integral parts of the actuator can be divided into mainly Three parts.

- Fixture
- Gears
- Stepper motor and Controller

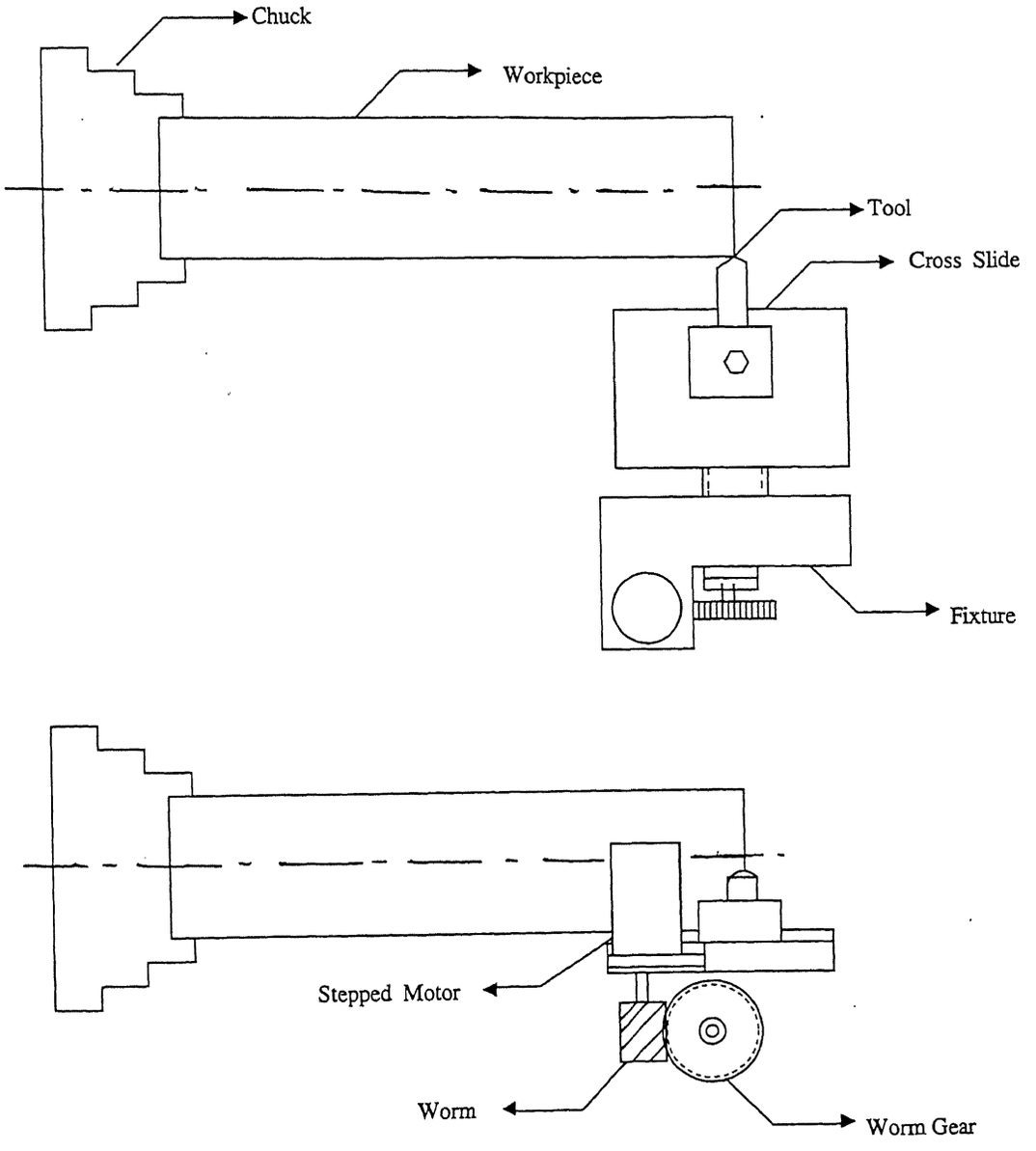

Figure 2.11: The Actuator

2.4.1 Fixture

The fixture is made of the mild steel and it is designed so as to hold the stepper motor and gears arrangement.

The fixture was designed and fabricated by taking care of the following points.

- It should be rigid and compact, and should not cause any vibration.
- It should not bend with the load of the stepper motor.
- It should be easy to remove or rearrange so as to conduct the experiments.

2.4.2 Worm Gears

The worm gears are used whenever there is a need of high reduction in the speed as in the present work. The least count of the cross slide micrometer is 0.05 mm. In order to decrease this least count up to microns worm gear was designed and fabricated. The worm gear and wheel are designed by considering the limiting factors as center distance between them and the number of teeth on worm gear. Here the center distance is 105 mm and the number of teeth is 68.

2.4.3 Stepper Motor and Controller

Stepper motor is a special type of motor in which angular motion can be easily controlled. A controller gives output to a driver system which amplifies the sequence signal to the required level. A series of predefined sequence controls the motion of the motor. Each step in the sequence advances the motor by one step. For the presently used stepper motor one step is equal to 1.8 of degree angular motion. Thus 200 steps correspond to one revolution of the motor. Following the sequence in reverse direction the motor is reversed. The stepper motor also can function in the half-step mode. In the present work the half step mode sequence was used. The maximum torque carrying capacity of the stepper motor is 21 kg-cm and it is capable of moving the cross slide even at the cutting conditions. The stepper motor is controlled by a controller using a logical input. The logical input should be 15 volts in parallel format. For PC, an interfacing circuit was designed. Details of which are discussed in the next paragraph.

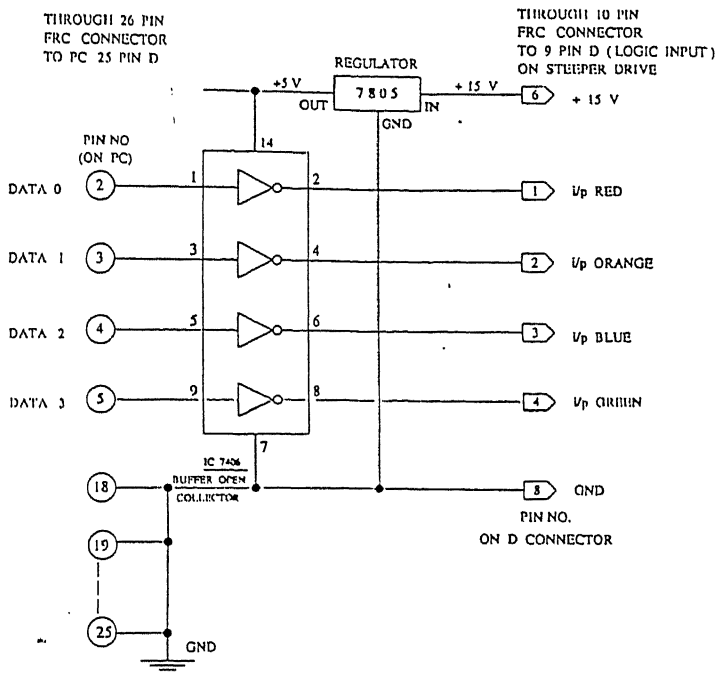

Figure 2.12: PC Interfacing Circuit

2.4.4 PC Interfacing Circuit

The PC interfacing with the controller of the stepper is done by designing an interfacing circuit. The designed circuit takes the input from the printer port.

Here the decimal value is sent with some time lag from the printer port to PCIC where the sequence of signal gets added to the buffer voltage and becomes +15 V from +5 V. This signal is then sent to the logic input of the motor controller. For communication with the logic unit of the stepper motor controller, a parallel communication is desirable. Due to this reason printer port has been selected for parallel communication.

The schematic diagram of the final setup is shown in the Fig. 2.13 The photographs of the set-up are shown in Fig. 2.14 and Fig. 2.15.

2.5 Planning of experiments

The main aim of the experiments is to collect the flank wear data at different working conditions to train the neural network. Along with the experiments are also required for testing the fabricated sensor. For doing the experiments the planning of experiments is

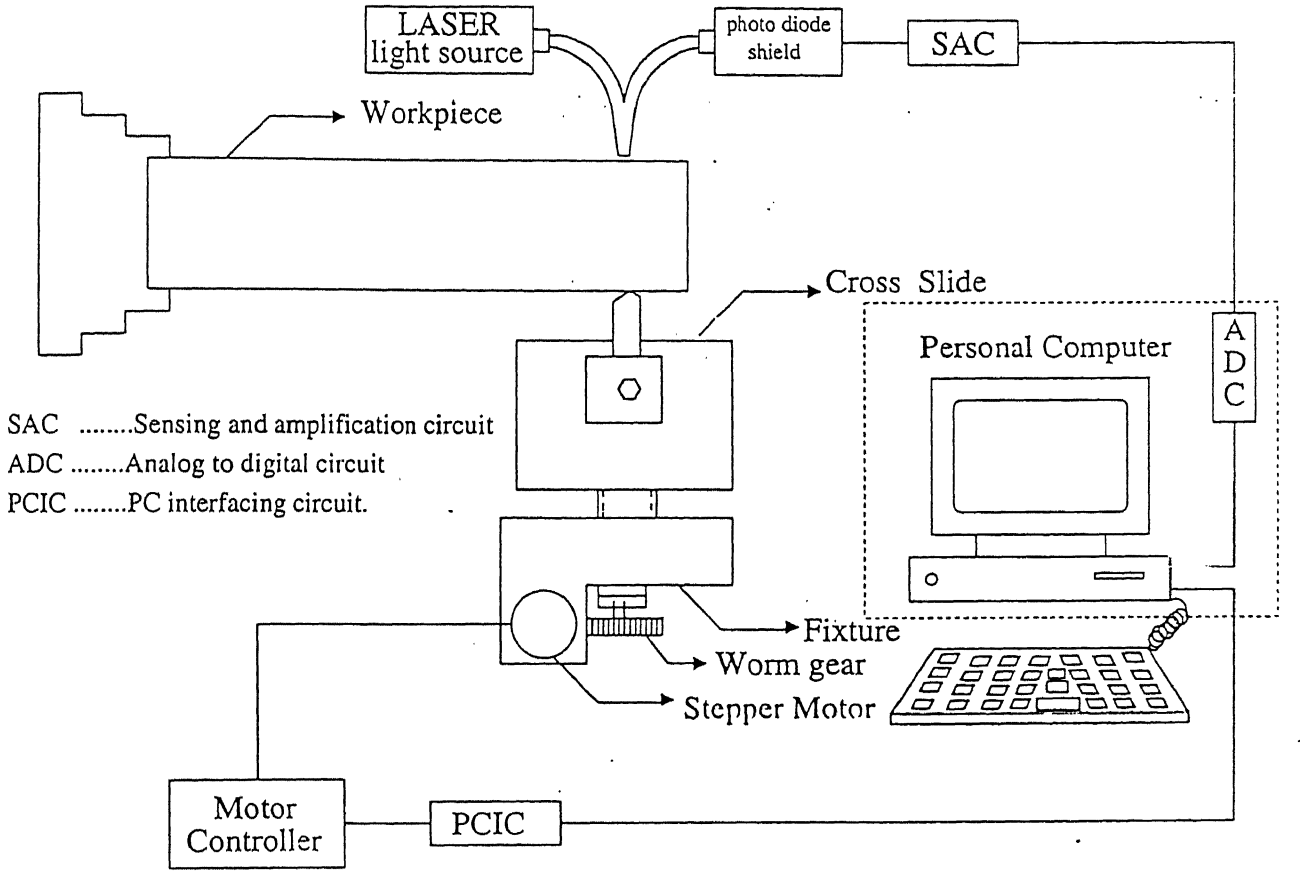

Figure 2.13: The Set up arranged for conducting experiments.

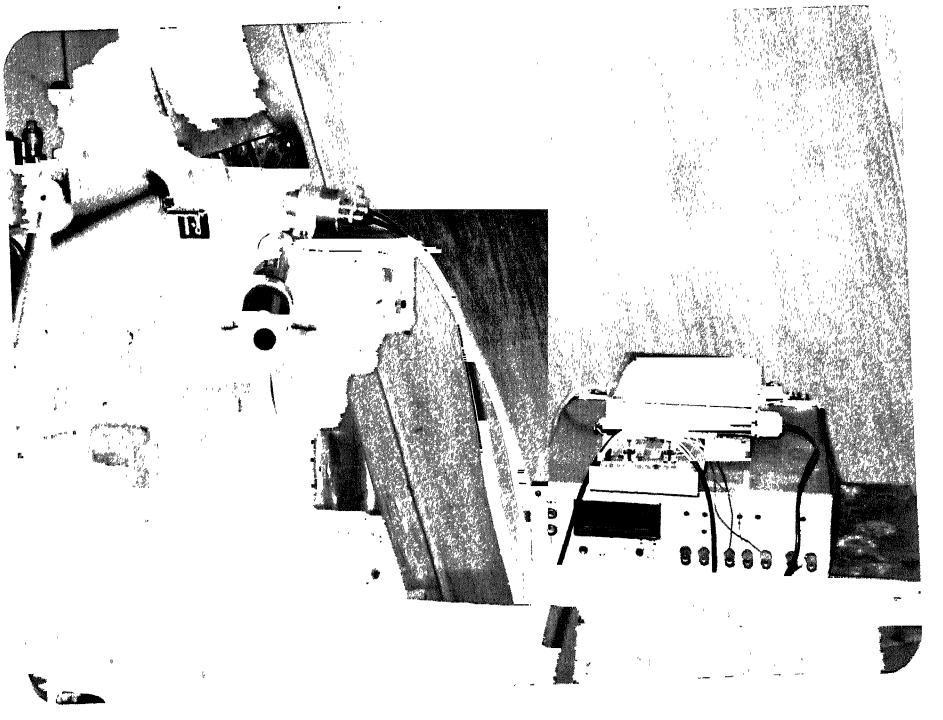

Figure 2.14: Photograph showing the final setup.

Figure 2.15: Another photograph showing the final setup.

done. The Planning of experiments is introduced to fulfill the following requirements:

- To get the training data. for neural networks, uniformly from all the regions of working area.
- To reduce the total number of experiments.
- To conduct parametric study.

If all the factors represent the quantitative variables like, temperature, time, speed etc., the response, y, can be written as a function of the levels of these variables[14].

$$\begin{aligned} y_u &= \phi(x_{1u}, x_{2u}, \ldots, x_{ku}) + e_u \\ where, u &= 1,\ 2,\ \ldots,\ N \end{aligned}$$

where, N is the total number of observations in a particular experiment

$$\begin{aligned} x_{iu} &= \textit{the level of } i_{th} \textit{ factor in the } u_{th} \textit{ observation} \\ e_u &= \textit{experimental error of the } u^{th} \textit{ observation} \\ and, &\quad \textit{function } \phi \textit{ is called the response surface} \end{aligned}$$

A knowledge of the function, ϕ, gives a complete summary of the results of the experiment. These experimental design can be developed for fitting the polynomials of first or second order.

The fitting of polynomials can be treated as a particular case of the multiple linear regression. The relation between y_u and x_{iu} is of the form :

$$y_u = \beta_0 x_{0u} + \beta_1 x_{1u} + \cdots + \beta_k x_{ku} + e_u$$

where, k is the total number of variables

The two way array of x_{iu} is called the X matrix and the column of y_u values is called the Y vector.

The least squares estimate b_i of the β_i so as to minimize the sum of squares of the deviations.

$$\sum_{u=1}^{N} (y_u - b_0 x_{0u} - b_1 x_{1u} - \cdots - b_k x_{ku})^2$$

The values of b_i, which minimize this expression, satisfy the normal equations

$$\begin{aligned} b_0(00) + b_1(01) + \cdots + b_k(0k) &= (0y) \\ \vdots \qquad \vdots \qquad\qquad \vdots &= \vdots \\ b_0(k0) + b_1(k1) + \cdots + b_k(kk) &= (ky) \end{aligned}$$

where,

$$
\begin{aligned}
(ij) = (ji) &= \sum_{u=1}^{N} x_{iu}\, x_{ju} \\
&= \textit{sum of the products of the } i_{th} \textit{ and } j_{th} \textit{ column in } X \\
(ii) &= \sum_{u=1}^{N} x_{iu}^2 \\
&= \textit{sum of the squares of the } i^{th} \textit{ column in } X \\
(iy) &= \sum_{u=1}^{N} x_{iu}\, y_u \\
&= \textit{sum of the products of the } i_{th} \textit{ column in } X \textit{ with } Y
\end{aligned}
$$

Although the normal equation can be solved directly, it is useful to calculate the set of intermediate quantities, C_{ji}, (inverse matrix).

The regression coefficients b_i are obtained as

$$
\begin{aligned}
b_i &= \sum_{j=0}^{k} C_{ji}\,(jy) \\
&= \textit{sum of the product of } i^{th} \textit{ column of } C_{ji} \textit{ with the column } (jy)
\end{aligned}
$$

Residual sum of squares:

$$R_k = yy - \sum_{i=0}^{k} b_i(iy)$$

Residual mean square:

$$S^2 = \frac{R_k}{N-k-1} \qquad (2.4)$$

These normal equations are easy to solve, when the variables x_{iu} are mutually orthogonal. In this case, all sum of the products (ji) vanish $(i \neq j)$ and the normal equation reduces to:

$$
\begin{aligned}
(ii)\, b_i &= (iy) \\
\textit{and, } b_i &= \frac{iy}{ii} \\
\textit{and, inverse matrix, } C_{ji} &= \frac{1}{ii};\ C_{ji} = 0,\ i \neq j
\end{aligned}
$$

2.5.1 Central composite rotatable design for three factors

This design is used, normally, in the following conditions, when

- No linear relationship between the input and the output variables exists.

- More than two levels are required for each of the input variables.
- Repeatability of the experiments is quite good.

As these conditions are largely satisfied in the present case, Therefore, this design has been used.

The general form of a quadratic polynomial for three variables is illustrated as:

$$\begin{aligned} y_u &= b_{0u} + b_{1u}x_1 + b_{2u}x_2 + b_{3u}x_3 + b_{11u}x_1^2 \\ &\quad + b_{22u}x_2^2 + b_{33u}x_3^2 + b_{12u}x_1x_2 + b_{13u}x_1x_3 + b_{23u}x_2x_3 \end{aligned} \tag{2.5}$$

In order to estimate these coefficients (b_{0u}, b_{1u}, ..., b_{23u}), x_{iu} must take at-least three different levels. This suggests the use of the factorial designs of 3^k series. One disadvantage of 3^k series, however, is that the number of experiments become quite large. Therefore, some researchers[14], constructed the composite design by adding some more combinations to the 2^k series. If the coded levels of each x-variable are -1 and 1, then in 2^k factorial, the additional factor combination are given as:

$$(0,\ 0,\ 0);\ (-\alpha,\ 0,\ 0);\ (\alpha,\ 0,\ 0);\ (0,\ -\alpha,\ 0);\ \cdots;\ (0,\ 0,\ \alpha)$$

The value of α can be chosen to make the regression coefficients, orthogonal to one another, or to minimize the bias that is created, if the true form of response surface is not quadratic.

The researchers[14], also pointed out that for a rotatable design the value of α must be $2^{k/4}$. Therefore, for the three level design, value of α is given as:

$$\alpha = 2^{3/4} = 1.682 \tag{2.6}$$

In the present design, actually, the five levels ($-\alpha$, -1, 0, 1, α), of x-variable are used. Substituting the value of α from Eq. 2.6, the levels are given as:

$$(-1.682,\ -1,\ 0,\ 1,\ 1.682)$$

The complete design is shown in the Table 2.1. The columns headed x_1, x_2 *and* x_3, specify the actual combination to be used. The x_1^2, x_2^2 *and* x_3^2, shows the squared terms and x_1x_2, x_1x_3 *and* x_2x_3, shows the cross product terms, of the general quadratic equation given in the Eq. 2.5. the corresponding values of the y is placed on the right.

Now the sums of each products of each column in X matrix with the column of y values are denoted by $(0y)$, $(1y)$, $(2y)$, and so on.

x_0	x_1	x_2	x_3	x_1^2	x_2^2	x_3^2	x_1x_2	x_1x_3	x_2x_3	y
1	-1	-1	-1	1	1	1	1	1	1	-
1	1	-1	-1	1	1	1	-1	-1	1	-
1	-1	1	-1	1	1	1	-1	1	-1	-
1	1	1	-1	1	1	1	1	-1	-1	-
1	-1	-1	1	1	1	1	1	-1	-1	-
1	1	-1	1	1	1	1	-1	1	-1	-
1	-1	1	1	1	1	1	-1	-1	1	-
1	1	1	1	1	1	1	1	1	1	-
1	-1.682	0	0	2.828	0	0	0	0	0	-
1	1.682	0	0	2.828	0	0	0	0	0	-
1	0	-1.682	0	0	2.828	0	0	0	0	-
1	0	1.682	0	0	2.828	0	0	0	0	-
1	0	0	-1.682	0	0	2.828	0	0	0	-
1	0	0	1.682	0	0	2.828	0	0	0	-
1	0	0	0	0	0	0	0	0	0	-
1	0	0	0	0	0	0	0	0	0	-
1	0	0	0	0	0	0	0	0	0	-
1	0	0	0	0	0	0	0	0	0	-
1	0	0	0	0	0	0	0	0	0	-
1	0	0	0	0	0	0	0	0	0	-

Table 2.1: central composite rotatable design for three factors

From the values of $(0y)$, $(1y)$ *etc.*, the regression coefficients are computed by the equation given as:

$$\begin{aligned} b_0 &= 0.166338\ (0y) - .056791\ \Sigma\ (iiy) \\ b_i &= .073224\ (iy) \\ b_{ii} &= .0625\ (iiy) + .006889\ \Sigma\ (iiy) - .056791\ (0y) \\ b_{ij} &= .125\ (ijy) \end{aligned} \tag{2.7}$$

Where, the only auxiliary quantity needed is $(\Sigma\ (iiy))$, which can be found out by adding the cross products of all the squared terms with y *i.e.*

$$\Sigma\ (iiy) = (11y) + (22y) + (33y)$$

Substituting these values of the regression coefficients in Eq. 2.5, the response y, can easily be found out.

The range of input cutting parameters were decided, on the basis of data given in the handbooks, machine capabilities and the practical experience as:

$$\begin{aligned} cutting\ velocity &= 20 - 70\ m/min \\ feed\ rate &= 0.05 - 2.5\ mm/rev \\ depth\ of\ cut &= 0.4 - 0.9\ mm \end{aligned}$$

To reduce the total number of experiments and to get the data uniformly from all the regions of the selected working area, the design of experiments procedure is adopted as discussed above. In the present case, Central composite rotatable design for three factors, has been used. The three factors, are cutting speed, feed and depth of cut. These factors were identified as most effecting factors in flank wear phenomenon. In this design, there are five levels associated with each factor. The input parametric values are scaled, according to these five levels, which are given in Table 2.2.

level	cutting velocity,v (m/min)	feed rate,f (mm/rev)	depth of cut, d (mm)
-1.682	21.4	.063	.4
-1	31.0	.100	.5
0	45.0	.150	.65
1	59.0	.2	.8
1.682	68.0	.225	.9

Table 2.2: Different level of cutting parameters

Chapter 3

SYSTEM DEVELOPMENT

The sensor system consists of a fiber optic sensor with an amplification circuit and the control system consists of a stepper motor and a controller with a PC interfacing circuit. The system sends an analog signal in the form of a voltage. This signal corresponds to the diameter of the workpiece at that particular instant. The difference between the initial signal(taken when the machining starts) and instantaneous signal corresponds to the change in the diameter of the workpiece at that particular instant. If this change is more than a certain predefined threshold value(explained in later sections) then the controlling system is activated to control the tool post(tool) for minimizing the dimensional inaccuracy. In order to compare the previous stored value with the particular instantaneous value, there is a need of system which can integrate these two different hardware set-ups. This can be performed by having a flexible system and a logic device. The required system was designed and developed using the software technology. The present chapter describes the design and development of the software part for the sensor. The sensor requires a logical device which can compare the previously stored value (reference value)with the instantaneous value and gives the signal to the stepper motor controller. To decrease the errors and increase the flexibility personal computer was used for this purpose. The PC is with Intel microprocessor chip. The software was developed for various tasks using the C language due to its special advantages in the hardware control.

The system developed consists of three different modules.

- Sensing module,
- Controlling module and
- Operating module

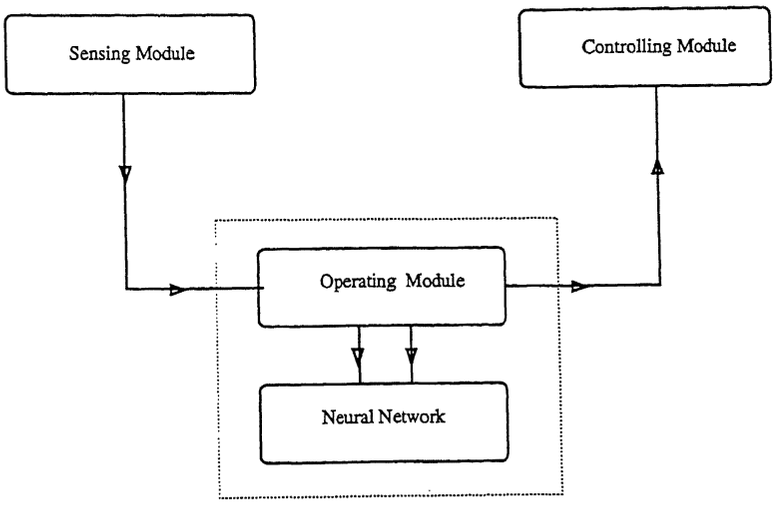

Figure 3.1: Software Architecture

The figure 3.1 shows the software architecture.

3.1 Sensing Module

The sensing module percepts the analog signal and converts it to the corresponding digital value. Initially the sensing module is called by the operating module. This module first cleans the address of the ADC card and then checks for proper switch setting on the card. Following are the arguments(information) that are required for the sensing module

- Number of conversions and
- Channel number from which the signal has to be sensed.

The signal is sensed by a software trigger which was stored in the dardy register. This signal is added to a variable *Avg*. The same procedure is followed for the value entered for the number of conversions. Finally the average value(Avg/Number of conversions) is

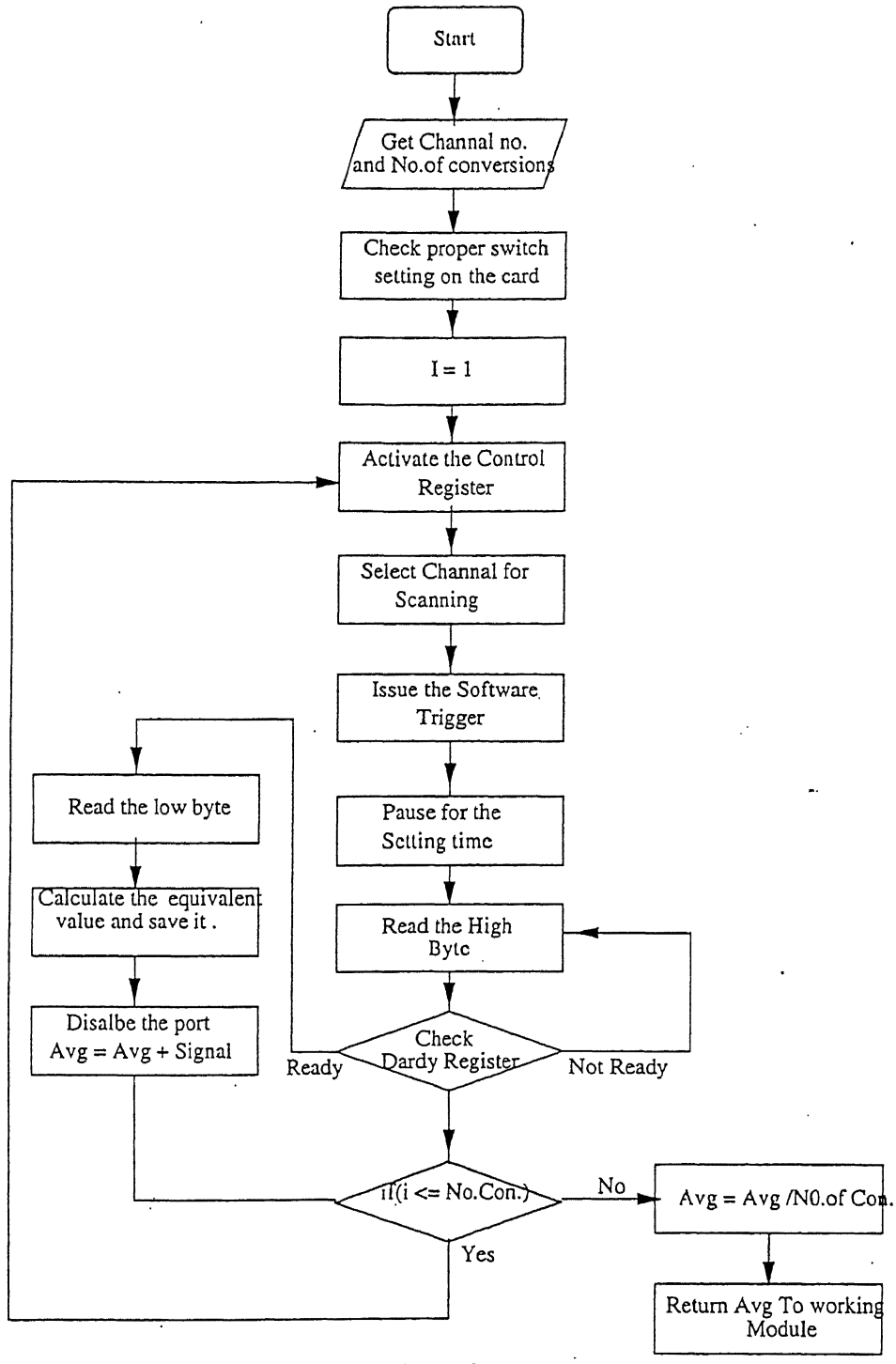

Figure 3.2: Flow Chart of the Sensing Module

returned from the sensing module to the operating module. Figure 3.2 shows the flow chart of the sensing module.

3.2 Controlling Module

The controlling module is for controlling the stepper motor according to the signal obtained from the operating module. The sequence of bits are sent from the printer port to the PC interfacing circuit. PC interfacing circuit increases its voltage from 5 V to 15 V

controller requires 15 V. The controlling module takes some arguments(information) from the operating module. The arguments are

- Number of steps to be moved.
- Mode of operation .(Half or full mode of operation)
- Backward operation or Forward operation.

The sequence of signals in table 2.1 consists of the sequences of bits and their corresponding decimal values. This decimal value is converted into a hexadecimal value. These values are sent from the printer port by using low level command in the C language with some time lag between each signal. The least time lag possible is 4 milli seconds. In the present work the least value is used. The details about the hardware control using software command in C language are given in the Appendix 1. The figure 3.3 shows the flow chart of the Controlling Module.

3.3 Operating Module

The operating module is the main module which receives and sends the information to sensing module and the controlling module. As the machining starts, keyboard interrupt is issued to start the working of the operating module. First it will clear the printer port and port of the ADC card. Then this module gets the signal from the sensing module and considers it as reference. Later it will take the signal again and checks with the reference. If the change in voltage is greater than prescribed threshold value which depends upon the precision of the job(this value entered by the operator to the computer. This value corresponds to the allowed dimensional inaccuracy of the job.) to be produced and the ~~front~~ slope of the characteristic curve of the optical sensor as shown in the figure 2.3, the operating module will give the corresponding signal to the controlling module to compensate the tool wear. For the present work, the slope of the characteristic curve was 3.33 V/mm and the precision entered was 0.03mm . The full details about the present working conditions are given in the next chapter and reasons are also given for taking the precision as 0.03 mm. The operating module also displays the change in voltage and number of signals given for compensation .

The system works interactively to display the flank wear on the VDU. It also warns the user whenever the flank wear reaches the some predefined value. The flow chart of the operating module is shown in the figure 3.3. In the flow chart the variable $dvdx$

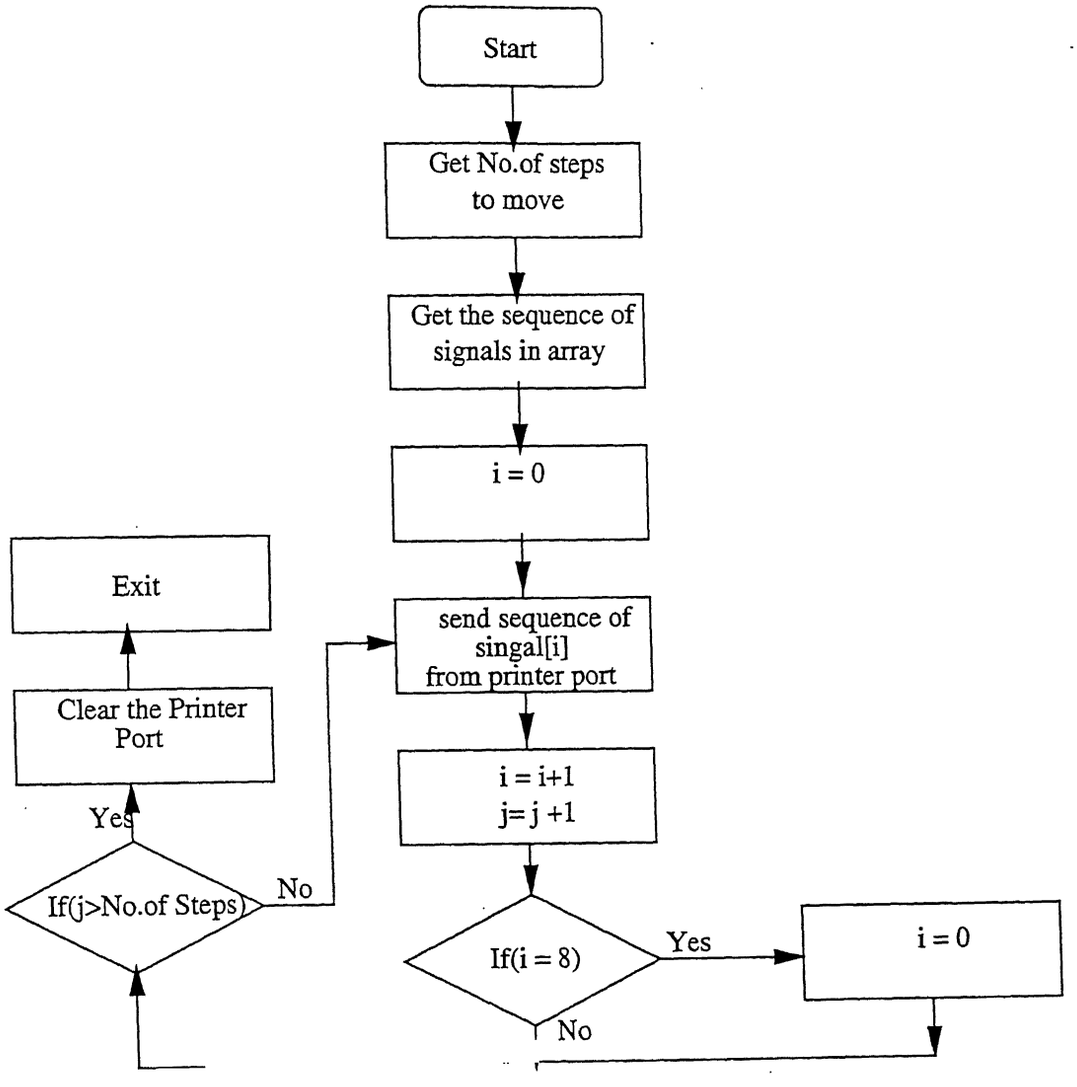

Figure 3.3: Flowchart of Controlling Module

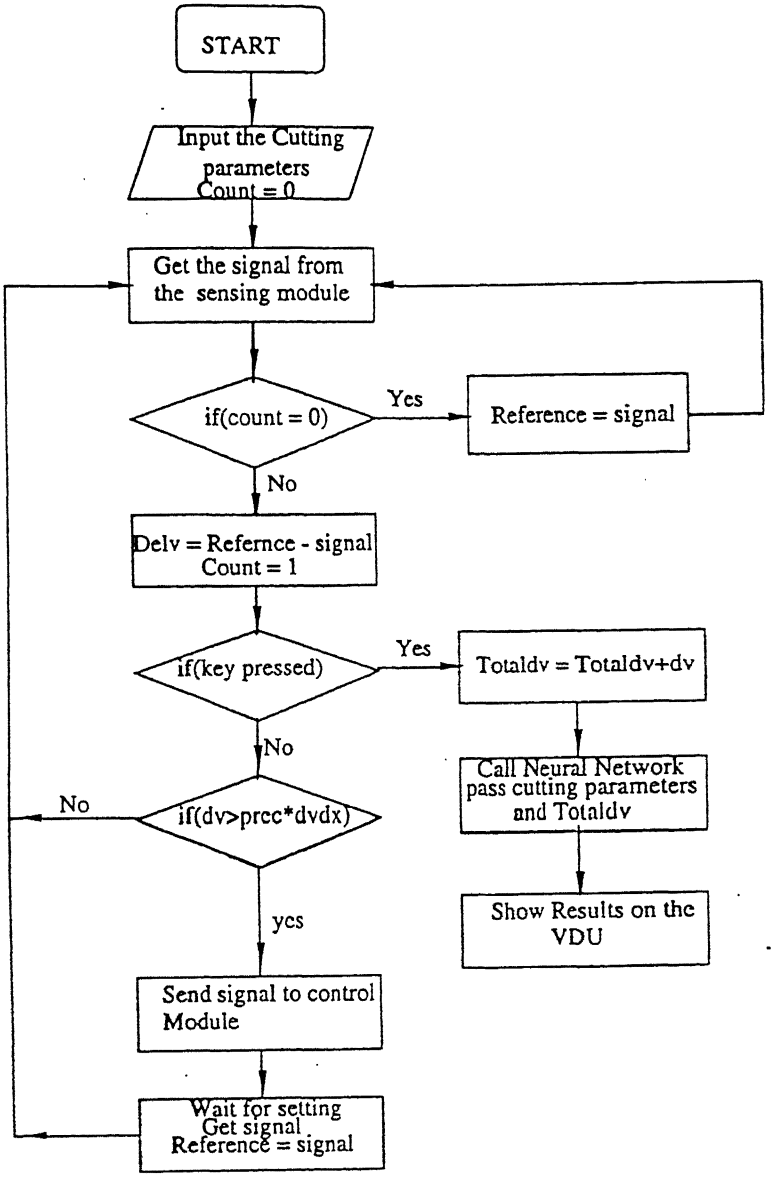

Figure 3.4: Flowchart of Operating Module

represents the slope of the characteristic curve of the optical sensor(figure 2.3c). The prediction of the flank wear in the present work is done by a special technique called **Neural network**. The Neural networks part in the present work comes under operating module. The following paragraphs briefly describe the theory of the neural networks and how it has been developed for the present problem.

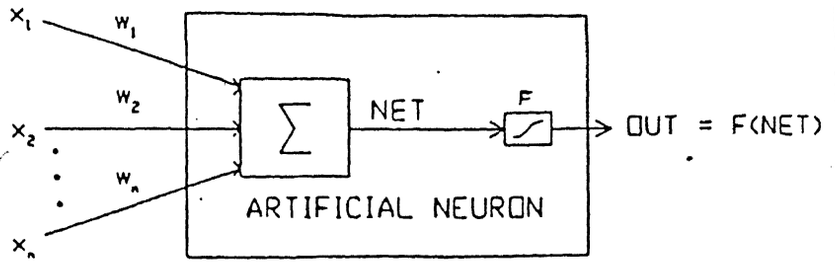

Figure 3.5: Artificial Neuron with the activation function [13]

3.4 Neural Networks

3.4.1 Introduction

Artificial Neural networks are inspired from the biological science and works in the similar way as biological neurons works. These elements are then organized in a way that they are analogous to the human brain. Artificial neural networks exhibit a surprising number of the brain's characteristics.

The electro chemical signals are transmitted by biological neurons over neural pathways and each neuron receives signals from other neurons through special junctions called synapses. Some inputs tend to excite the neuron, while others tend to inhibit them. When the cumulative effect exceeds some threshold value, the neurons fires, and sends a signal down to other neurons. An artificial neuron simulates these simple biological characteristics of the neuron and works in the same way. Due to various advantages, lot of research is taking place to develop this technology. Generally the artificial neural networks are used in face recognition and the development of new systems in the various fields like Aero Space etc., In neural networks, each artificial neuron receives a set of inputs and each input is multiplied by a weight analogous to synaptic strength. The sum of all weighted inputs determines the degree of firing called the activation level and is further processed by an activation function which may be a threshold function or a smooth sigmoidal function, also called nonlinear function. An artificial neuron with such an activation is shown in the Fig 3.5. Construction of a neural network involves the following tasks[13]:

- to determine the network properties consisting of the network topology. (connectivity), the type of connections, the order of connections, and the weight range.
- to determine the node properties like the activation range and the activation function
- to determine the system dynamics, *i.e.*, the weight initialization scheme, the acti-

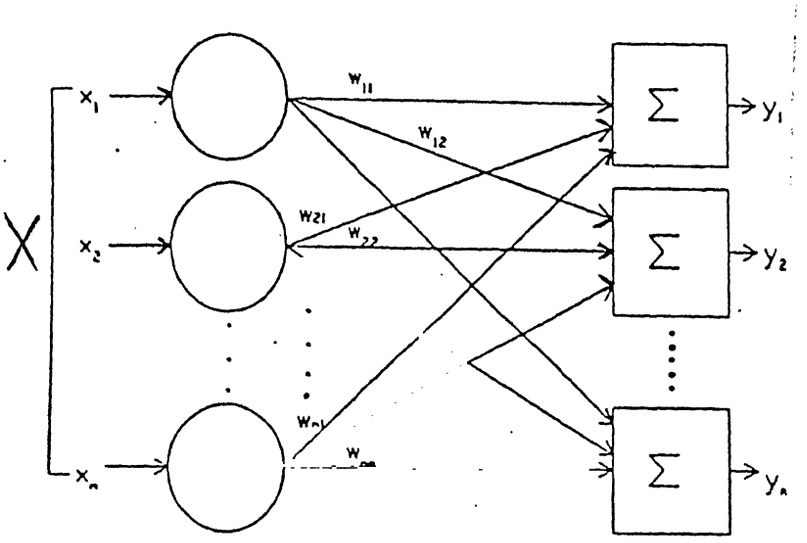

Figure 3.6: Single layer neural network [13]

vation calculating formula and the learning rule.

An artificial neural network can be considered as a network of many simple processors (units), each possibly having a (small amount of) local memory. The units being connected by communication channels (connections) which usually carry numeric (as opposed to symbolic) data. The units operate only on their local data and on the inputs they receive via the connections between them. The design motivation is what distinguishes neural networks from other mathematical techniques, A neural network is a processing device, either an algorithm, or actual hardware whose design was motivated by the design and functioning of human brains and components thereof. It can consist of one or more layers. A single layer and a two layer neural networks are shown in the Fig 3.6 and Fig 3.7 respectively.

Generally the neural networks will follow some sort of training rule whereby the weights of the interconnections are adjusted on the basis of the presented patterns. The neural networks learn from the past experiences and exhibits some structural capabilities for generalization. Learning is the process by which the free parameters of a neural network are adapted through a continuous process of stimulation by the environment in which the network is embedded. The type of learning is determined by the manner in which the parameter changes take place. The neural networks perform better if it learns from more patterns. The error between the predicted and the real values can be minimized by more number of input pattern data.

In general, a neural network consists of several processors, each of which is connected

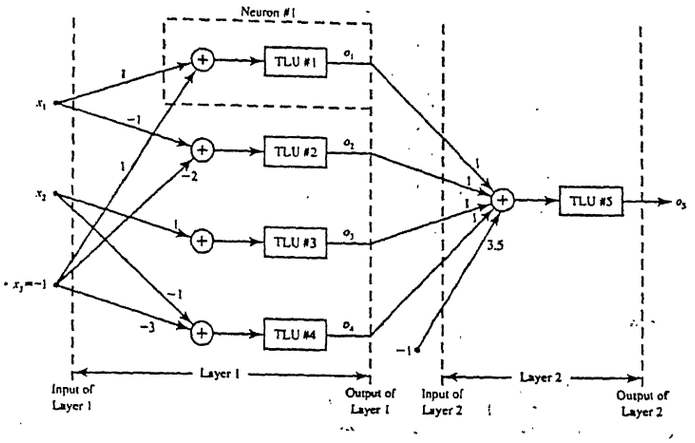

Figure 3.7: Double layer neural network [13]

to all other nodes. In the present work, however, only layered feed-forward network has been used. Use of such a layered structure sacrifices some amount of parallelism, since only processors in the same layer operate in parallel, but adjacent layer compute serially. Although some parallelism is lost, these networks are popular, because there exists a sophisticated learning scheme for training the network[13].

A threshold value is associated with each of the nodes. The output of each node is determined by the level of the input signal in relation to the threshold value. Signals can propagate through the network only between the adjacent layers and only in the single direction. These signals are modified by connection strengths (weights) between the nodes.

Let,

$$\begin{aligned} t_{ik} &= \textit{threshold of the } i^{th} \textit{ node in the } k^{th} \textit{layer} \\ w_{i,j,k} &= \textit{Weight between the } j^{th} \textit{ node in } (k-1)^{th} \textit{ layer} \\ &\quad \textit{to the } i^{th} \textit{ node in the } k^{th} \textit{ layer} \\ net_{i,k} &= \textit{input to the } i^{th} \textit{ node in } k^{th} \textit{ layer} \\ O_{i,k} &= \textit{output of the } i^{th} \textit{ node in } k^{th} \textit{ layer} \end{aligned}$$

Then the input to a node is,

$$net_{i,k} = \sum_{j} [w_{i,j,k} O_{j,k-1}] + t_{i,k}$$

The summation index, j, extends over all nodes in the $(k-1)^{th}$ layer. The output of a

node, therefore, can be rewritten as,

$$O_{i,k} = f(net_{i,k})$$

where, in general, f,is non-decreasing function of the input of the node. It has been seen[15]

1. a positive weight between two units implies the excitation of one unit by the other, and
2. a negative weight implies inhibition (nodes contradict each other).
3. A zero weight implies that the units do not affect each other directly.

The function f can take-on several forms. For a linear network,

$$O_{i,k} = net_{i,k}$$

The most frequently used functions are the threshold and the sigmoid functions, given by:

$$\begin{aligned} f(net_{i,k}) &= 1 \ \ if \ net_{i,k} > 0 \\ &= 0 \ \ otherwise \\ f(net_{i,k}) &= \frac{1}{1+e^{-net_{i,k}}} \end{aligned}$$

Another commonly used activation function is the hyperbolic tangent. It is similar in shape to the logistic function and is expressed as:

$$f(net_{i,k}) = \tanh(x)$$

Both of the functions have been shown in the Fig 3.8, Like the logistic function, the hyperbolic tangent function is S shaped, and it is symmetrical about the origin, resulting in:

$$f(net_{i,k}) = 0 \ when, \ net_{i,k} = 0$$

Unlike logistic function, the hyperbolic tangent function has a bipolar value for $f(net_{i,k})$, a characteristic that has been shown to be beneficial in certain networks.

Due to these reasons, the hyperbolic tangent function has widely been used and is used in the present work also.

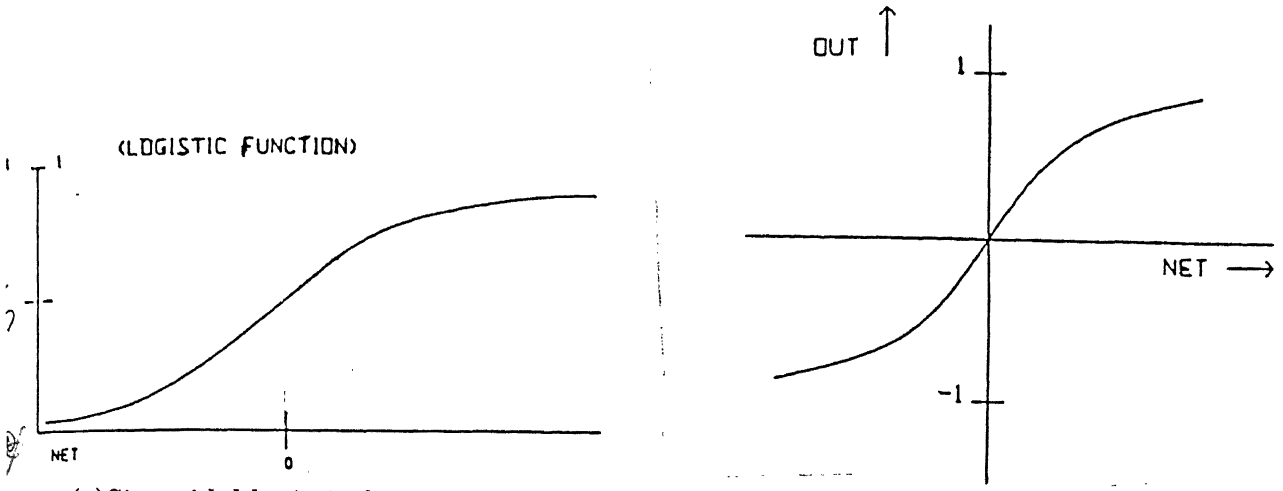

(a)Sigmoidal logistic function (b)Hyperbolic tangent function

Figure 3.8: The activation functions [13]

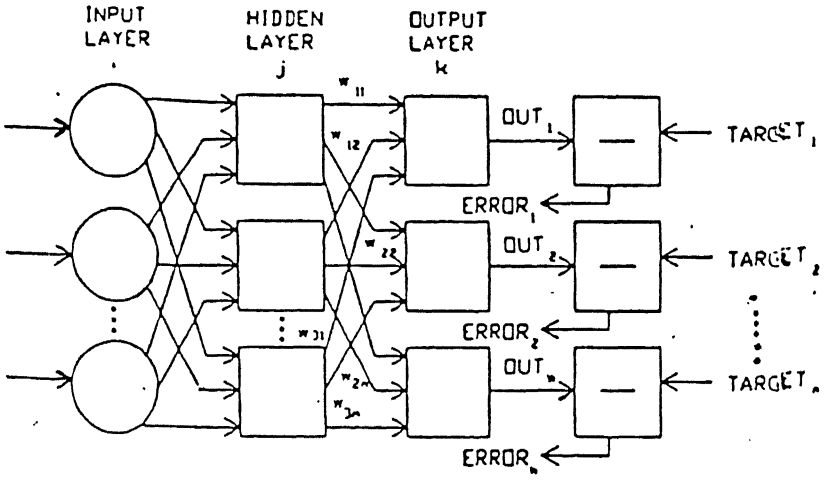

Figure 3.9: Two layer back propagation network [13]

3.5 Learning of Neural Network

For many years, there was no theoretical sound algorithm, for training the multi-layer artificial neural network. Single layer networks provided severe limitations in their way of representation and their way of learning.

The invention of back propagation algorithm has played a crucial role in the development of the neural networks. Back propagation is a systematic method for training the multi-layer artificial neural networks, which has a strong mathematical foundation.(Fig 3.9) The objective of training the network is to adjust the weights, so that the application of a set of inputs produces the desired set of outputs. For the sake of simplicity, these input-output sets can be referred to as vectors. Training assumes that each

input vector is paired with a target (output) vector, together these are called a training pair.

Before starting the training process, all the weights must be initialized to the small numbers. This ensures that the network is not saturated by large values of the weights and prevents certain other discrepancies, e.g. if the weights start at equal values and the desired performance requires unequal values, then the network will not learn.

The following steps have been required to train the back-propagation network, which can easily be understood with the help of Fig 3.9.

1. Select the next training pair from the training set, apply the input vector to the network input.
2. Calculate the output of the network.
3. Calculate the error between the network output and the desired output (the target vector from the training pair).
4. Adjust the weights of the network in a way, that minimizes the error.
5. Repeat the steps 1 to 4 for each vector in the training set until the error for the entire set is acceptably low.

It may be seen that steps 1 and 2 constitute a forward pass in that the signal propagates from the network input to its output. Steps 3 and 4 constitute a reverse pass. Here the calculated error signal propagates backward through the network, where it is used to adjust the weights. These two passes are now expanded and expressed in somewhat more mathematical form.

3.5.1 Forward pass

In forward pass, the weights remain unchanged throughout the network and the function signals are computed on neuron-by-neuron basis. Specifically, the function signal appearing at the output of neuron, j, in n^{th} iteration, is computed as:

$$y_j = \phi(v_j) \tag{3.1}$$

where, v_j is the net internal activity level of neuron, j, defined as

$$v_j = \sum_{i=1}^{p} w_{ji}\, y_i \tag{3.2}$$

where, p is the total number of inputs applied to the neuron, i, and w_{ji} is the weight connecting the neuron, i, to the neuron, j, and y_i is the input signal of the neuron, j, or equivalently, the function signal appearing at the i^{th} neuron.

The error signal at the output of neuron, j, is defined as:

$$e_j = d_j - y_j \tag{3.3}$$

where, d_j, is the desired output.

The half of sum of squared errors is obtained as:

$$E = \frac{1}{2} \sum_{j=1}^{r} e_j^2 \tag{3.4}$$

where, r, is the total number of neurons in the output layer.

3.5.2 Reverse pass

The reverse pass starts at the output layer by passing the error signal leftward through the network, layer by layer and recursively calculating the local gradient, δ, for each neuron. The weights are changed in accordance with the delta rule as explained in the following paragraphs.

Adjusting the weights of the output layer

In back propagation algorithm the weights of the output layer are adjusted as shown in the Fig 3.10. A correction $\Delta w_{ji}(n)$ is applied to the weights, which is proportional to the instantaneous gradient, expressed as:

$$\frac{\partial E}{\partial w_{ji}} = \frac{\partial E}{\partial e_j} \frac{\partial e_j}{\partial y_j} \frac{\partial y_j}{\partial v_j} \frac{\partial v_j}{\partial w_{ji}}$$

From Eq. 3.4

$$\frac{\partial E}{\partial e_j} = e_j$$

From Eq. 3.3

$$\frac{\partial e_j}{\partial y_j} = -1$$

From Eq. 3.1

$$\frac{\partial y_j}{\partial v_j} = \phi\prime(v_j)$$

From Eq. 3.2

$$\frac{\partial v_j}{w_{ji}} = y_i$$

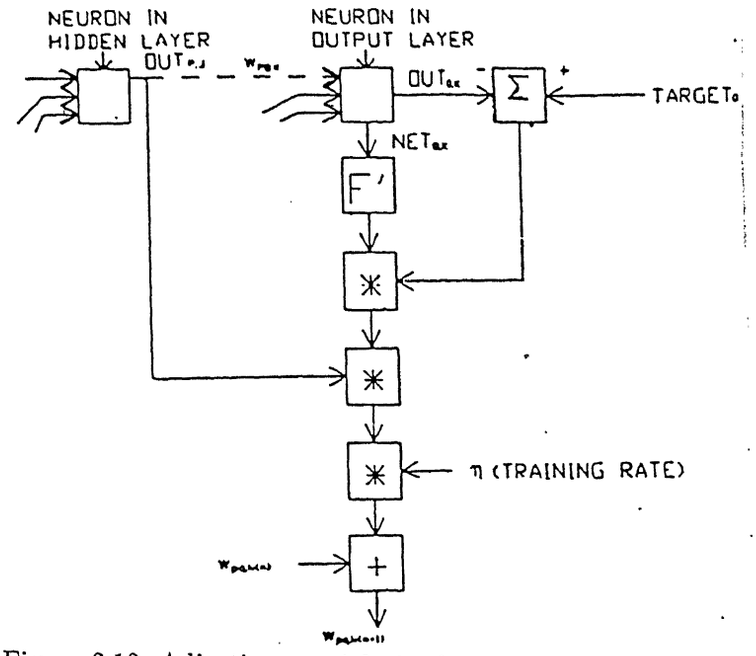

Figure 3.10: Adjusting a weight in the output layer. [13]

$$Therefore,\ \frac{\partial E}{\partial w_{ji}} = -e_j\ \phi\prime(v_j)\ y_i$$

The correction applied according to the delta rule is

$$\Delta w_{ji} = -\eta\ \frac{\partial E}{\partial w_{ji}}$$

where, η = learning rate parameter This factorη is very influencing parameter. If this is taken as large value then the system may not learn at all. If it less then the learning time increases and takes more computational time.

$$Therefore,\ \Delta w_{ji} = \eta\ \delta_j\ y_i$$

where the local gradient is

$$\delta_j = e_j\ \phi\prime(v_j) \tag{3.5}$$

$$\begin{aligned} Now,\ \phi(v_j) &= a\ \tanh(bv_j) \\ &= a\ \frac{1-\ exp\ (-bv_j)}{1+\ exp\ (-bv_j)} \\ &= \frac{2a}{1+\ exp\ (-bv_j)} - a \end{aligned}$$

$$\begin{aligned} \Rightarrow\ \phi\prime(v_j) &= \frac{2ab\ exp\ (-bv_j)}{(1+\ exp\ (-bv_j))^2} \\ &= \frac{2ab}{1+\exp\ (-bv_j)}(1-\ \frac{1}{1+\ exp\ (-bv_j)}) \\ &= b\ (a+\phi(v_j))\ (1-\ \frac{a+\phi(v_j)}{2a}) \\ &= \frac{b}{2a}\ (a+\phi(v_j))\ (a-\phi(v_j)) \end{aligned}$$

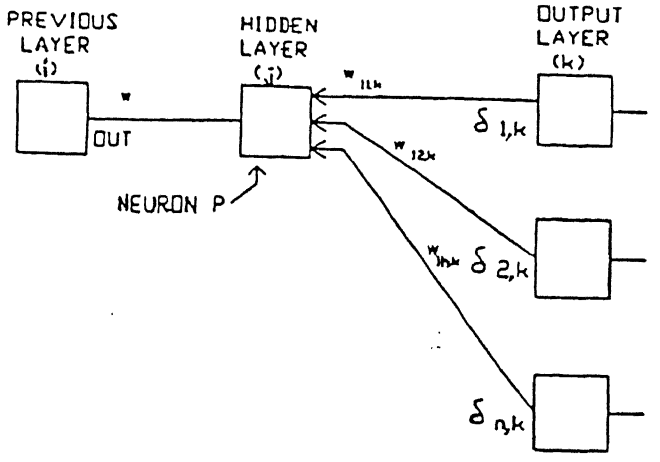

Figure 3.11: Adjusting a weight in the hidden layer [13]

$$= \frac{b}{2a}\left(a^2 - \phi^2\left(v_j\right)\right)$$
$$= \frac{b}{2a}\left(a^2 - y_j^2\right)$$

Adjusting the weights of the hidden layer

Hidden layers have no target vector, so the training process described above can not be used for these layers. This lack of training targets, makes the training extremely difficult. Back propagation trains the hidden layer by propagating the output error back through the network, layer by layer, adjusting the weights at each layer. The process has been shown in the Fig 3.11. Equation are used for all layers, both input and output. However, for hidden layer, δ, must be generated without the benefit of a training vector.

From Eq. 3.5

$$\delta_j = -\frac{\delta E}{\delta y_j}\frac{\delta y_j}{\delta v_j}$$
$$= -\frac{\delta E}{\delta y_j}\phi\prime(v_j)$$

From Eq. 3.4

$$\frac{\delta E}{\delta y_j} = \sum_k e_k \frac{\delta e_k}{\delta y_j}$$

$$= \sum_k e_k \frac{\delta e_k}{\delta v_k} \frac{\delta v_k}{\delta y_j}$$

Let, q is the total number of inputs fed to the neuron, k, in the hidden layer.

$$Since, e_k = d_k - y_k = d_k - \phi(v_k)$$

$$We\ have,\ \frac{\delta b_k}{\delta v_k} = -\phi\prime(v_k)$$

$$and\ since,\ v_k = \sum_{j=0}^{q} w_{kj}\ y_i$$

$$\Rightarrow \frac{\delta v_k}{\delta y_j} = w_{kj}$$

$$\frac{\delta E}{\delta y_j} = -\sum e_k\ \phi_k\prime[v_k - w_{kj}]$$
$$= -\sum \delta_k\ w_{kj}$$

Hence the local gradient for the hidden layer neurons can be written as:

$$\delta_j = \phi_j\prime v_j \sum_j \delta_k\ w_{kj}$$
$$= (\frac{b}{2a})\ (a^2 - y_j^2) \sum_j w_{kj}\ \delta_k$$

The program for neural network part involves the two separate parts. One part is for training which is written separately. The flow chart for this program is as shown in the figure 3.12 The second part is for predicting the wear of the tool which takes the input pattern which contains cutting speed, feed, depth of cut, voltage comes from the optical sensor. The second part is a part of the operating module as shown in the figure 3.13.

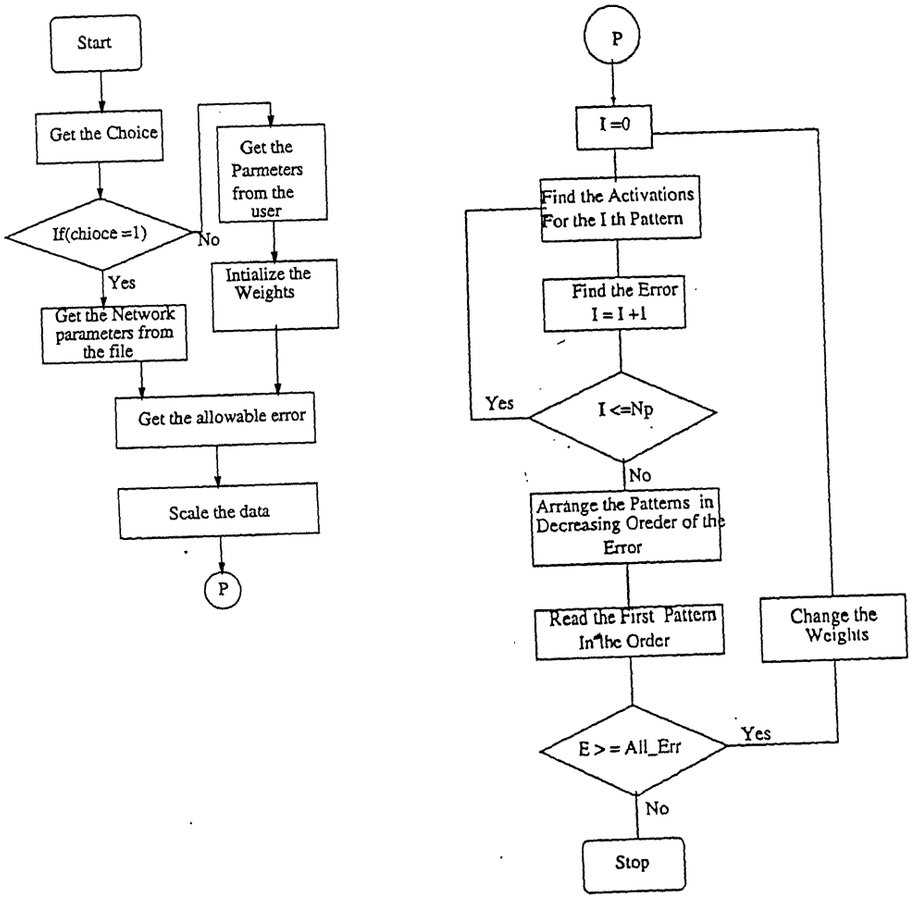

Figure 3.12: Flow Chart of the Neural Network for training

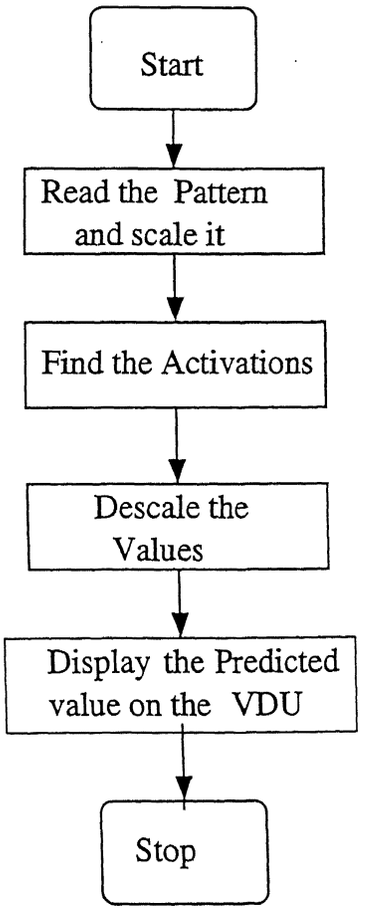

Figure 3.13: Flow Chart of the Neural Network for Predicting

Chapter 4

RESULTS AND DISCUSSION

The objective of the experiments carried out under different working conditions is to monitor the tool wear phenomenon during machining with feed back and without feed back system as well as to test the accuracy of prediction of the flank wear by trained neural network. For training the neural network the flank wear data was collected by conducting the experiments. For carrying out these experiments different procedures were adopted so as to avoid the errors. The experimentation can be divided mainly into three types.

- Type I :Experiments without feed back system,
- Type II :Experiments with feed back system and,
- Type III :Experiments to test the neural network system.

To get better results and to have repeatability of the experiments, tool material, work material, tool overhang, tool height, tool geometry (given in the appendix) were kept constant for all experiments as mentioned above. All the experiments were conducted on an engine lathe on which the sensor was mounted to monitor the tool wear and control the workpiece dimensional inaccuracy. The procedure adopted for conducting the experiments changes from type to type. The following paragraphs will give the full details of each type of the experiments.

4.1 Experiments Without feed back(Type I)

These experiments were carried out without feed back to investigate the dimensional instability of the job due to tool wear under different working conditions. The dimensional

instability of a job produced on the lathe can also be defined as diameter variation in the job achieved as compared to the desired diameter along the length of the workpiece. The workpiece length was taken as 30 cm. The design of experiments procedure was followed to plan these experiments. The total experiments conducted were 20 in number. The flank wear(h_f) was taken as the output response, and cutting speed, feed and depth of cut were taken as input variables. The complete plan of the experiments is given in table 2.2. The procedure for all these experiments is the same except that the cutting conditions change from experiment to experiment.

The procedure followed during experimentation was as follows.

- The machining was performed after setting all the cutting conditions that is, feed, cutting speed and depth of cut.
- After machining, the dial indicator whose least count is 0.002 mm was taken and placed on the carriage at the starting point of the machining and the dial was adjusted to indicate the zero reading.
- The dial indicator was moved by moving the carriage along the length of the workpiece and the readings at an interval of one cm length were noted down.
- The tool was removed from the tool post after machining and properly placed under the metallurgical microscope, with a scale on the eyepiece whose least count is 0.0635 mm. The flank wear was measured after cleaning the tool bit.

4.2 Experiments With Feed Back(Type II)

These experiments were carried out with feed back system by using the same cutting conditions with which the Type I experiments were carried out. The same methodology was followed for measuring the diameteral deviation of the workpiece and the flank wear.

The feed back system is made of optical sensor system and stepper motor with a controller. The optical sensor's characteristic curve were first found to get the optimum stand-off-distance. Using the experimental results, the following characteristic curves were obtained as shown in the figure 2.3. From the curves, the optimum range of stand-off-distance obtained as 2.5mm to 3.5 mm where the curve is almost linear. All the experiments (Type I ,II, III) were carried out by taking the stand-off-distance(SOD) as 3.0 mm. The bundle of fibers both receiving the light and carrying the light was placed to exactly coincide with the central axis of the workpiece as shown in the Fig. 4.1.

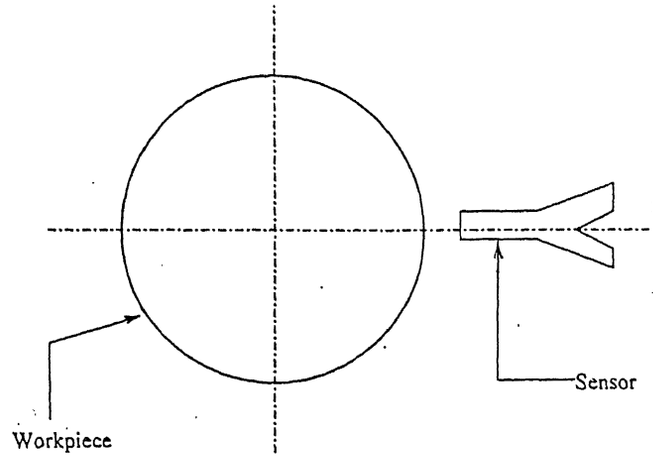

Figure 4.1: Workpiece and optical sensor arrangement.

The applied bias voltage to the photo diode was made almost constant to avoid fluctuations in the final signal obtained from the sensor.

Tool wear becomes measurable only after certain length of machining. The required measurable length is 10mm. Up to this length the maximum change of diameter of the workpiece is 0.012mm(0.006 mm for radius change) which is named as a correction factor. This correction factor (0.006mm) is added to the controlling movement signal which will be sent by the controlling module.

A change in the workpiece diameter and surface roughness leads a change in the voltage developed due to a change in the distance between the workpiece surface and the sensor. As the tool wears the workpiece diameter also changes accordingly and there will be a linear decrease in the voltage. The change in the voltage mainly corresponds to the change in the workpiece dimensions. The change in surface roughness also has a slight effect on the change in the voltage. Generally as the tool wears the surface roughness of the workpiece increases. The experiments were conducted to find this relationship. The Fig. 4.2 shows the relation between the sensor signal and the surface roughness drawn for the EN 24 steel as workpiece at the stand of distance 3.5mm.

This slope was used in the operating module with the variable dv_dx as shown in the flow chart of the operating module (fig.3.4).

The voltage signal read by the computer at a certain instant corresponds to the workpiece diameter at that location of the sensor. To find the average diameter at a particular instant n number of signals were taken along the workpiece circumference and a signal corresponding to the average value of all these n number of signals was sent to the op-

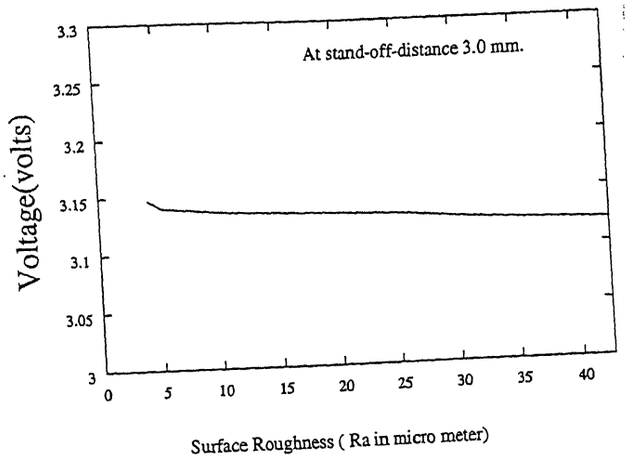

Figure 4.2: Variation of sensor output Vs Surface Roughness.

erating module. The number n is dependent upon the response time of the computer in sensing a voltage signal and the time for 1 revolution of the workpiece.

- Time taken for each signal to sense by the computer is 0.004 s and, the
- Time for 1 revolution of the workpiece is 60/N.

$$n = \frac{\frac{60}{N}}{0.004} \tag{4.1}$$

$$n = \frac{15000}{N} \tag{4.2}$$

$Where N = RPM\ of\ the\ Workpiece.$

The relation between the distance to be moved and number of controlling signals to be sent by the computer is found by finding the error in the cross slide by doing some experiments. With the results obtained there was an average error E as given below for each step. This error remained constant for a movement of the cross slide by more than 0.03mm. Due to this reason the precision of the job to be produced was taken as 0.03 mm.

$$E = 26.80 * 10^{-6} mm/step \tag{4.3}$$

This error is a positive error. The relation was derived as

$$z = \frac{n_c.p}{n_1.n_2} + E \tag{4.4}$$

where

n_c = *Number of signals to be sent to the controlling module.*

z= *Distance to be moved by the crossslide for n number of signals.*

p= *Pitch of the cross slide lead screw.*

n_1 = Number of teeth on the worm wheel.

n_2 = Number of steps moved by the stepper motor for one revolution of the motor shaft.

E = Error in the cross slide.

Finally by substituting the required values the final result is

$$n_c = 4981.z$$

The relation for n_c in terms of the z was used in the operating module to find out the number of signals to be sent to the controlling module.

With these conditions **twenty experiments** as designed were conducted as type I experiments. The flank wear for these 20 experiments was also noted and change in the workpiece diameter along its length of at an interval of 1cm increment was measured.

4.3 Results

The experiments were conducted with feed back and without feed back with the identical working conditions. They are numbered from 1 to 20 and arranged in the table according to composite rotatable design(table 3.4). The table 4.1 shows the flank wear with and without feed back system. The voltage corresponding to the dimensional inaccuracy was observed for the feed back system. The comparison of the dimensional inaccuracy with feed back and without feed back for various experiments is shown in figures from 4.3.1 to 4.3.20.

Figures 4.3.1 to 4.3.20 clearly show that the error in the measured workpiece diameter(in the Figures radius was shown) without feedback continuously increases along its length. However, the magnitude of the maximum error in each case is different, and it is a function of the machining conditions. Error in the radius(diameter) of the machined workpiece with feed back system increases along the length of the workpiece such that it is always below 0.03mm(0.06mm diameter change). This value was adopted as explained later.

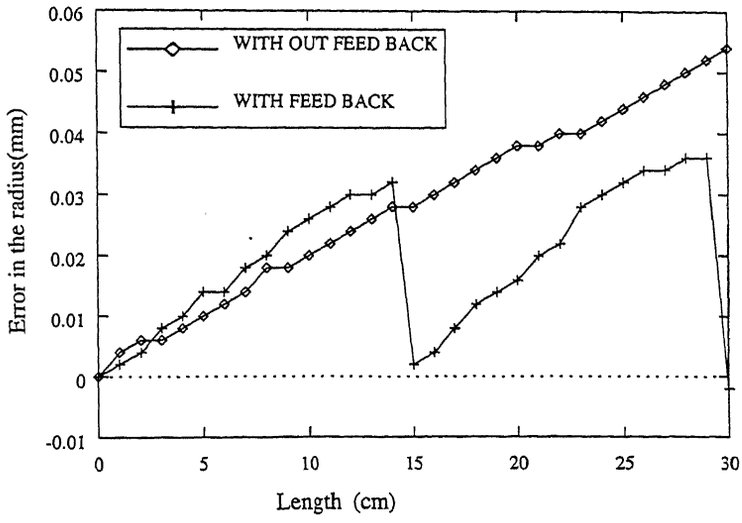

Fig.4.3.1 Experiment Number 1

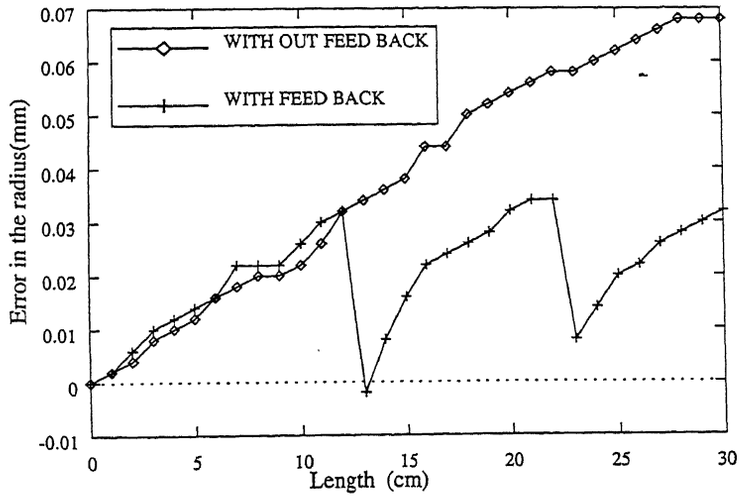

Fig.4.3.2 Experiment Number 2

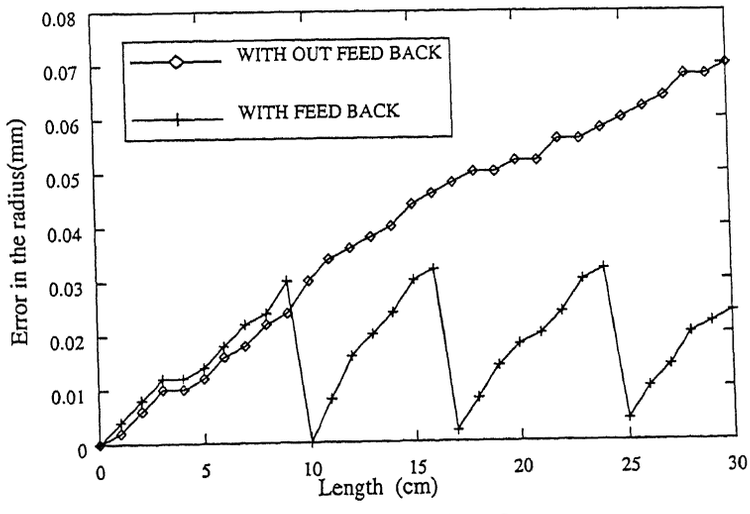

Fig.4.3.3 Experiment Number 3

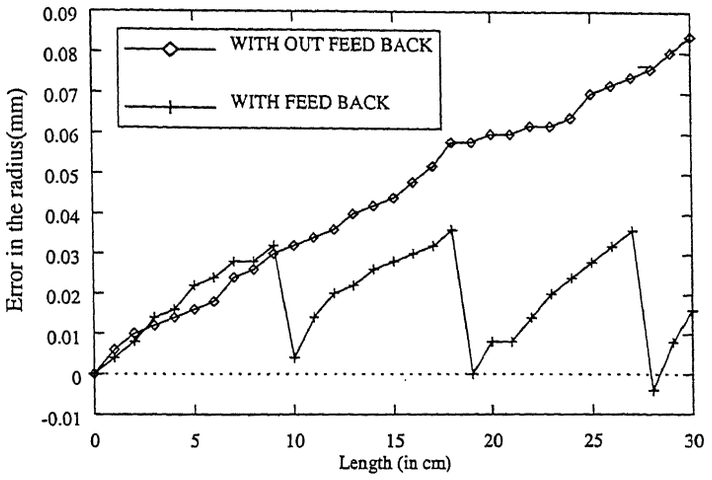

Fig.4.3.7. Experiment number 7

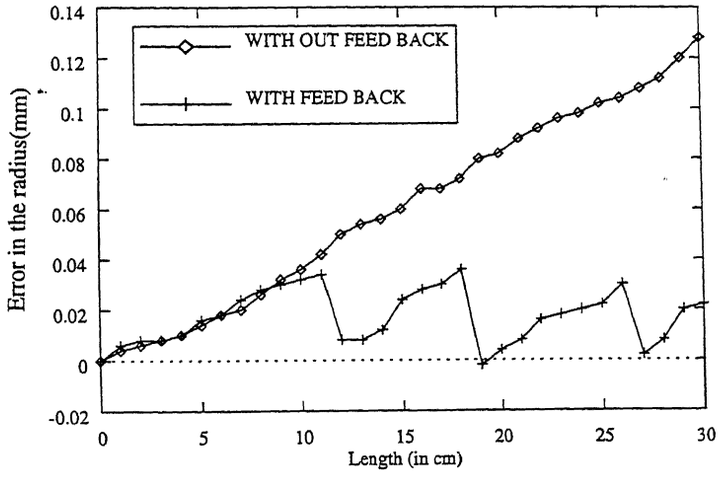

Fig.4.3.8 Experiment number 8

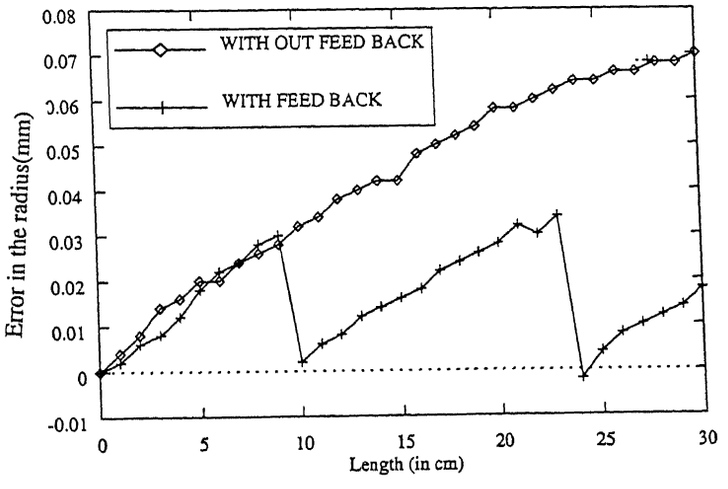

Fig.4.3.9 Experiment number 9

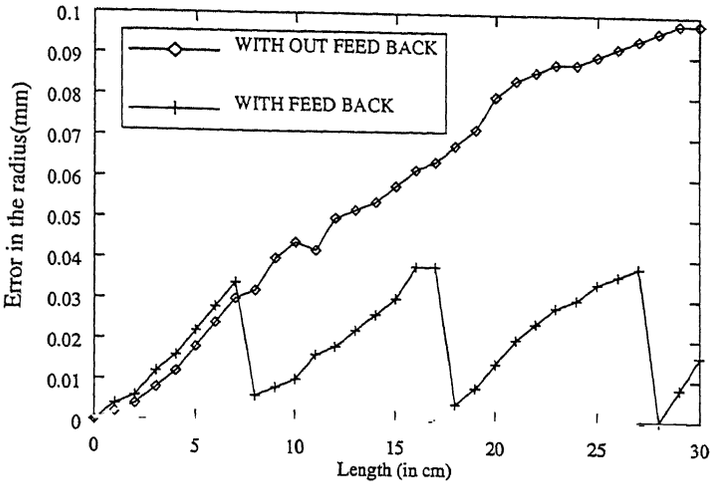

Fig.4.3.10 Eperiment Number 10

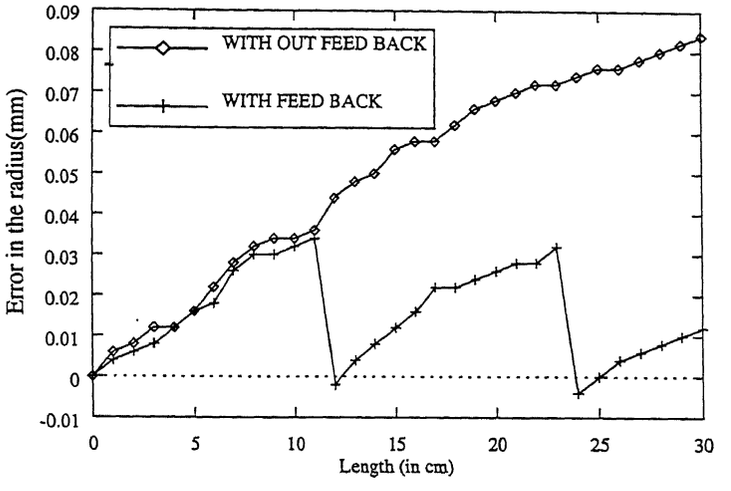

Fig.4.3.11 Eperiment Number 11

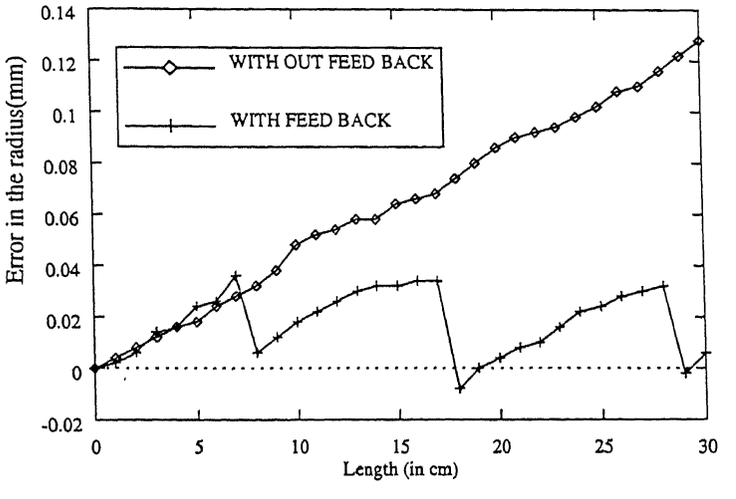

Fig.4.3.12 Eperiment Number 12

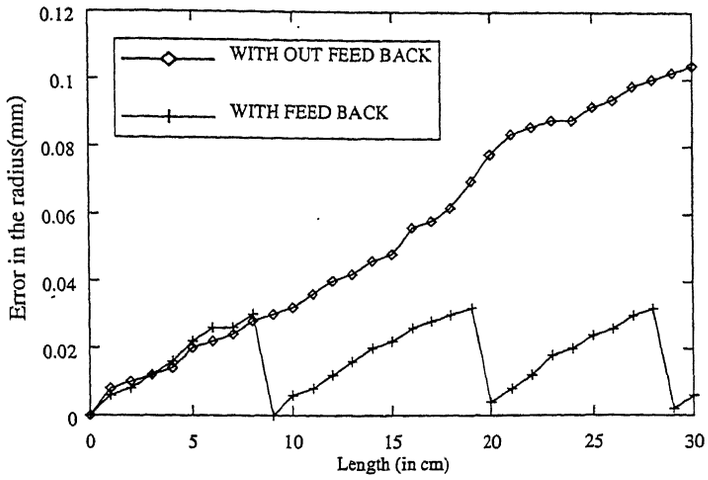

Fig.4.3.13 Experiment number 13

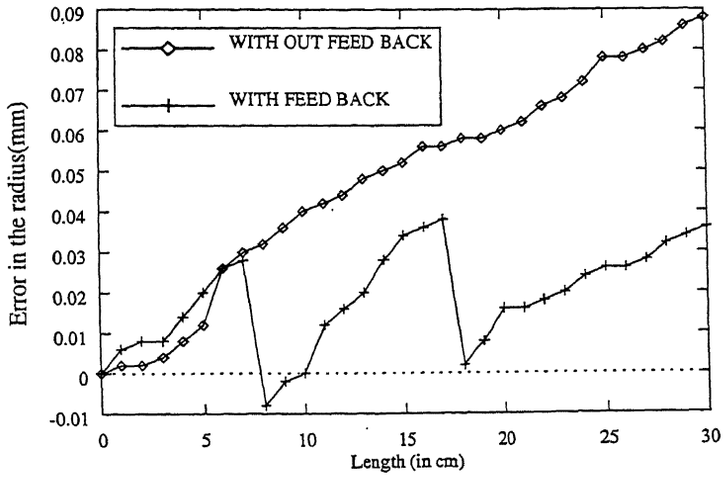

Fig.4.3.14 Experiment number 14

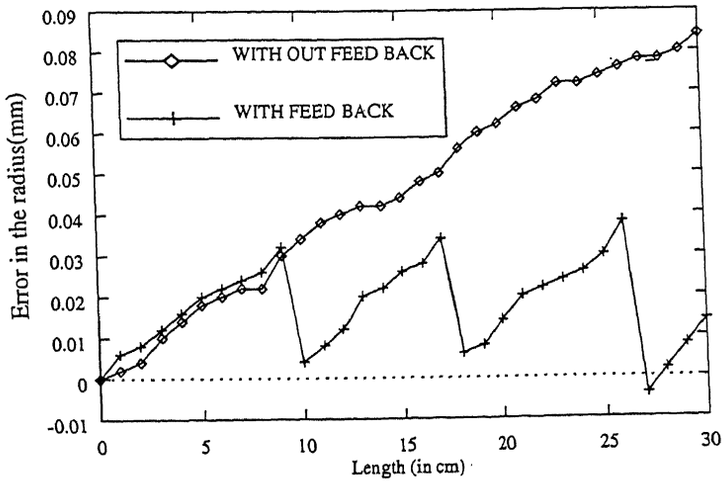

Fig.4.3.15 Experiment number 15

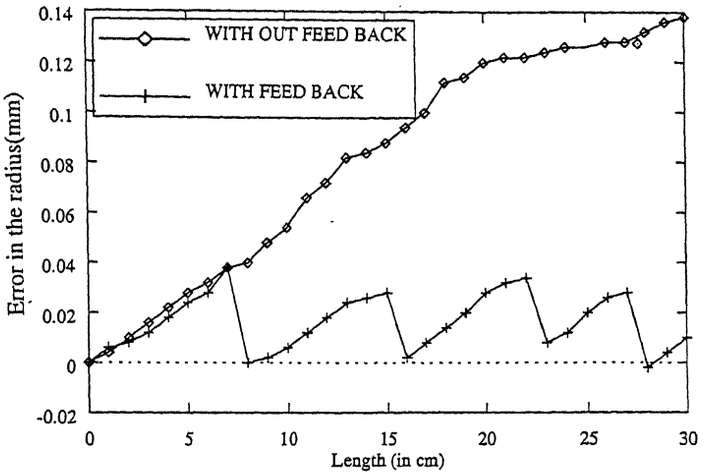

Fig.4.3.16 Experiment number 16

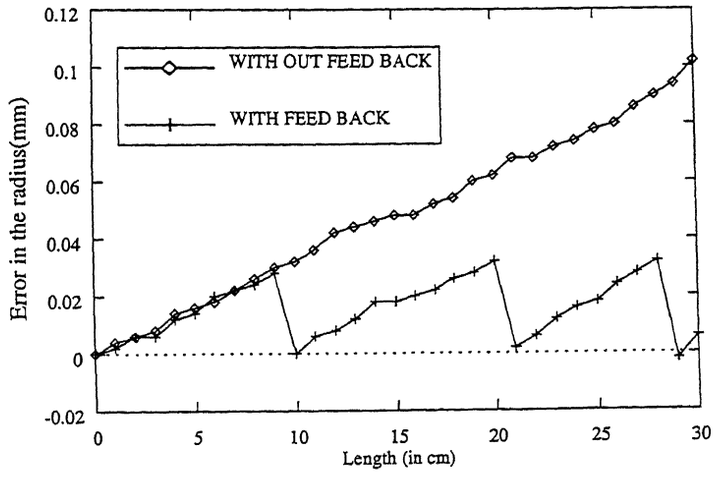

Fig.4.3.17 Experiment number 17

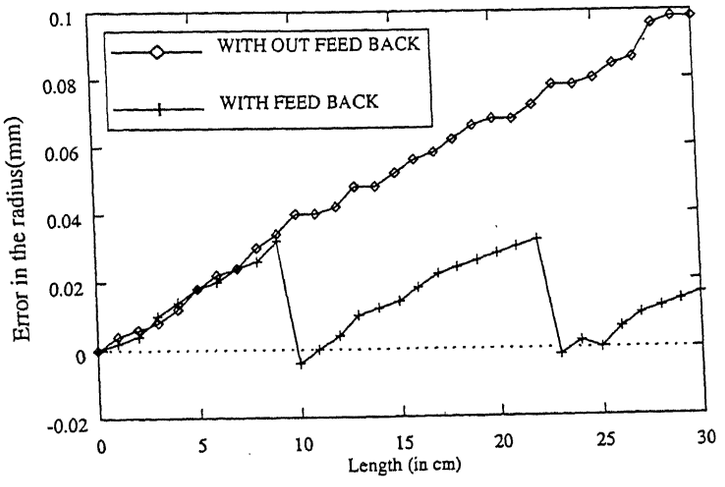

Fig 4.3.18 Experiment number 18

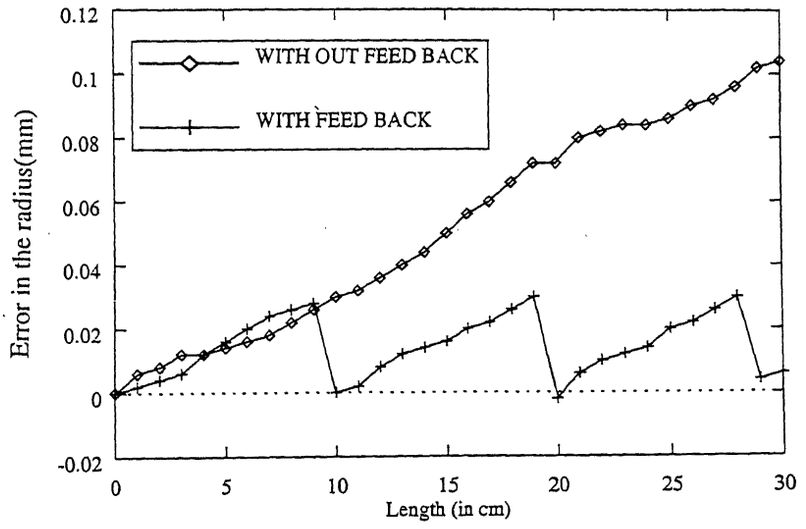

Fig.4.3.19. Experiment number 19

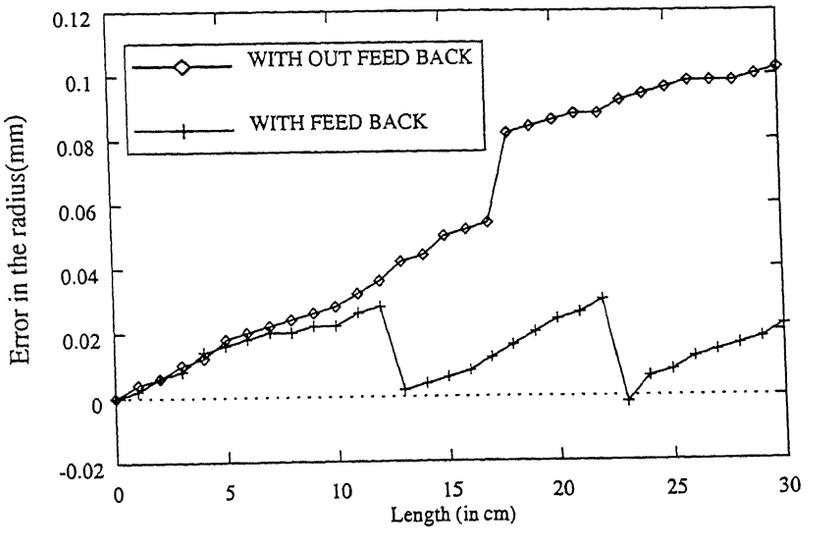

Fig.4.3.20. Experiment number 20

Figure 4.3: Comparison between the dimensional inaccuracy with FB and with out FB.

The flank wear with feed back system for different working conditions (table 4.2)was used as a training set for the neural network. The input vector for the neural network is cutting speed, feed rate, depth of cut, and voltage from the sensor. The output vector for the neural network is flankwear. With these data the neural network was trained until the allowable squared error between the predicted and the experimental values is equal to or less than 0.0009 which is defined by the operator. The training set of the neural network was given in the table 4.1.

After some threshold value of the error the learning time required by the system is more. For training the neural network, the number of neurons taken for input layer of the neural network was 4, for hidden layer 7 and for outer layer 1.

After learning of the neural network the training set was given as a input pattern and the prediction of the neural network was tested. Figure 4.5 shows the comparison of the experimental and predicted values.

Five experiments were conducted(Type III) with feed back system to test the trained neural network. The final voltage difference and the machining conditions were used as input pattern to the neural network subroutine in the operating module. The predicted values and measured valuesof the flank wear are shown in the Fig. 4.4.

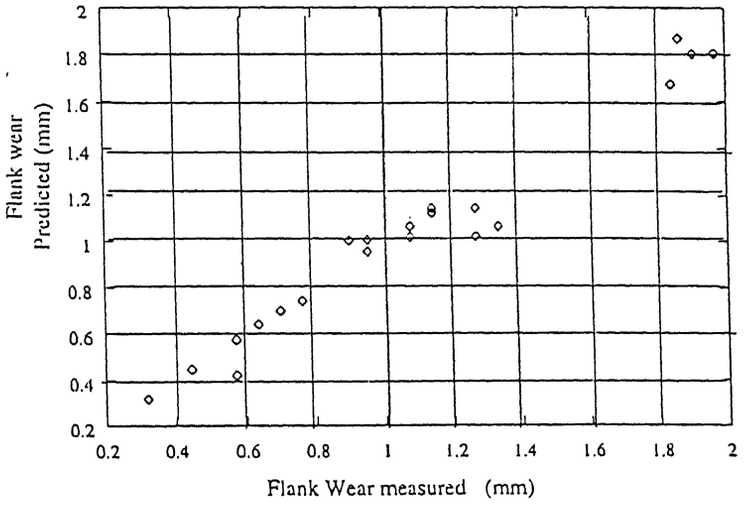

Figure 4.4: Comparison between the measured value and predicted value.

Exp.No	cutting velocity (m/min)	feed rate (mm/rev)	depth of cut (mm)	diference in voltage Volts	flankwear with FB mm	flank wear without FB mm
1	30.91	0.100	0.5	0.204	0.3175	0.1905
2	59.376	0.100	0.5	0.282	0.5715	0.3175
3	30.47	0.200	0.5	0.272	0.4450	0.381
4	58.30	0.200	0.5	0.314	1.1430	0.9525
5	31.90	0.100	0.8	0.291	0.9525	0.6985
6	60.31	0.100	0.8	0.486	1.9685	1.9685
7	31.73	0.200	0.8	0.279	0.6985	0.5715
8	59.96	0.200	0.8	0.383	1.8415	1.4605
9	21.31	0.150	0.65	0.235	0.7620	0.635
10	67.7	0.150	0.65	0.332	1.1430	0.762
11	44.76	0.060	0.65	0.228	0.5715	0.381
12	44.76	0.220	0.65	0.382	1.9050	1.5875
13	44.23	0.150	0.40	0.289	0.6350	0.5715
14	43.80	0.150	0.90	0.313	1.0795	0.6985
15	45.23	0.150	0.65	0.304	1.0795	0.9000
16	43.70	0.150	0.65	0.309	1.1430	1.143
17	46.40	0.150	0.65	0.309	1.0795	1.0795
18	43.22	0.150	0.65	0.291	1.1430	0.9525
19	46.80	0.150	0.65	0.293	0.9000	0.762
20	45.86	0.150	0.65	0.301	0.9525	0.8255

Table 4.1: The cutting conditions and results observed for tool

Exp.No	cutting velocity (m/min)	feed rate (mm/rev)	depth of cut (mm)	diference in Voltage Volts	flank wear With FB mm
1	30.91	0.100	0.5	0.204	0.3175
2	59.376	0.100	0.5	0.282	0.5715
3	30.47	0.200	0.5	0.272	0.4450
4	58.30	0.200	0.5	0.314	1.1430
5	31.90	0.100	0.8	0.291	0.9525
6	60.31	0.100	0.8	0.486	1.9685
7	31.73	0.200	0.8	0.279	0.6985
8	59.96	0.200	0.8	0.383	1.8415
9	21.31	0.150	0.65	0.235	0.7620
10	67.7	0.150	0.65	0.332	1.1430
11	44.76	0.060	0.65	0.228	0.5715
12	44.76	0.220	0.65	0.382	1.9050
13	44.23	0.150	0.40	0.289	0.6350
14	43.80	0.150	0.90	0.313	1.0795
15	45.23	0.150	0.65	0.304	1.0795
16	43.70	0.150	0.65	0.309	1.1430
17	46.40	0.150	0.65	0.309	1.0795
18	43.22	0.150	0.65	0.291	1.1430
19	46.80	0.150	0.65	0.293	0.9000
20	45.86	0.150	0.65	0.301	0.9525

Table 4.2: The Training Set for the Neural Network

S.No	cutting velocity (m/min)	feed rate (mm/rev)	depth of cut (mm)	diference in voltage (Volts)	flankwear mesured (mm)	flank wear predicted (mm)
1	65.97	0.150	0.6	0.280	1.270	1.1549
2	50.26	0.200	0.8	0.160	1.2065	1.2330
3	38.20	0.200	0.9	0.304	1.3335	1.2301
4	21.99	0.400	0.5	0.291	0.3810	0.3521
5	26.70	0.225	0.4	0.230	0.3810	0.3746

Table 4.3: The Verification Set of the Neural Network

Using the experimental data(Table 4.2) two polynomial equations in terms of the input variables have been evolved; One for the case with feed back and another without feed back. The response in both the cases was flank wear land. Evaluation of these response surface equations is simple and less time consuming as compared to neural network system. However the neural network can predict the response values with much less error whereas the statistical design of experiments will give a rough idea. The degree of the approximation depends upon various factors[14]. However the design of experiments can give a rough idea about the interrelation between various variables. Two different polynomials were obtained one for with out feed back and another for with feed back.

The polynomial is also called the *regressionequation*. In case of without feed back system the regression equation is given as

$$\begin{aligned} y \;=\; & +0.9388 + 0.12\,x_1 + 0.1625\,x_2 + 0.2248\,x_3 - 0.07433\,x_1^2 \\ & + 0.02672\,x_2^2 - 0.096790\,x_3^2 + 0.007937\,x_1x_2 - 0.182563\,x_1x_3 \\ & - 0.182562\,x_2x_3 \qquad (4.5) \end{aligned}$$

The regression equation for flank wear as response(y) and cutting parameters as variables for case with feed back system is given as

$$\begin{aligned} y \;=\; & +1.050 + 0.27\,x_1 + 0.1875\,x_2 + 0.2732\,x_3 - 0.03881\,x_1^2 \\ & + 0.06224\,x_2^2 - 0.07250\,x_3^2 + 0.0071375\,x_1x_2 + 0.1508\,x_1x_3 \\ & - 0.1350\,x_2x_3 \qquad (4.6) \end{aligned}$$

Here

In both the above equations 4.5 and 4.6

x_1 = cutting velocity

x_2 = feed rate

x_3 = depth of cut

y = Flank wear land (h_f)

4.4 Discussion

The main aim of the experiments is to collect the data for training the neural network and to test the efficacy of the sensor. The sensor is capable of sensing a gap above or equal to

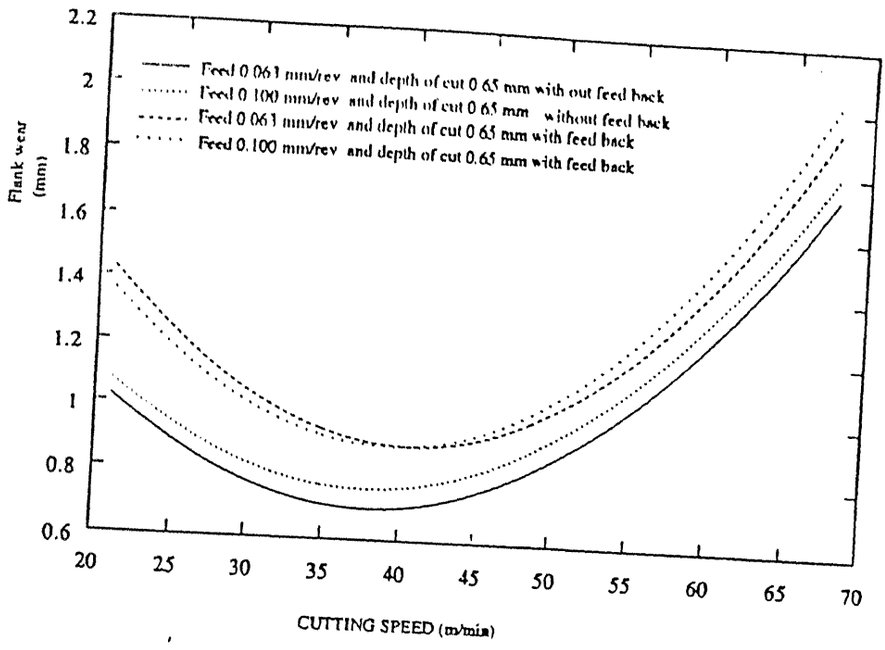

Figure 4.5: Variation of Flank wear Vs Cutting Speed with FB and without FB

20 μm with a tolerance of ± 4 microns. The feed back system also acting as controlling system, is capable to move the tool by not less than 0.03 mm. Hence, 0.03 mm precision was identified as the least possible controllable movement.

It is evident that the present system is effective only when the required dimensional inaccuracy is approximately equal to or more than 0.03mm. Although the sensor system is capable to sense 0.02 mm but the feed back system is not capable to do so. However such sensors can be easily adapted to CNC machines.[7]

The maximum flank wear was observed in case of FB system. This is due to additional abrasion wear of the tool. Whenever a compensation for the tool wear is made, its depth of cut increases resulting in the increased wear. This tool wear also depends upon the cutting speed. If the cutting speed is moderate or less then the rate of abrasion will be very small. At higher speeds there will be definitely increased tool wear with FB system. There must be a compromise between the additional tool wear and the dimensional inaccuracy that the FB is controlling. This can be achieved by operating the system at a moderate speed.

Various graphs were plotted using equations 4.5 to 4.6 to show the variation in the flank wear with different cutting conditions.

At low cutting speeds flank wear decreases as the cutting increases(fig. 4.5). However, beyond a certain value of cutting speed the flank wear starts increasing with the increase in the cutting speed, and this cutting speed is called as critical speed. The flank wear at low cutting speeds is mainly due to the attrition wear phenomenon. Attrition wear is not accelerated by high temperatures, and it tends to disappear at high cutting

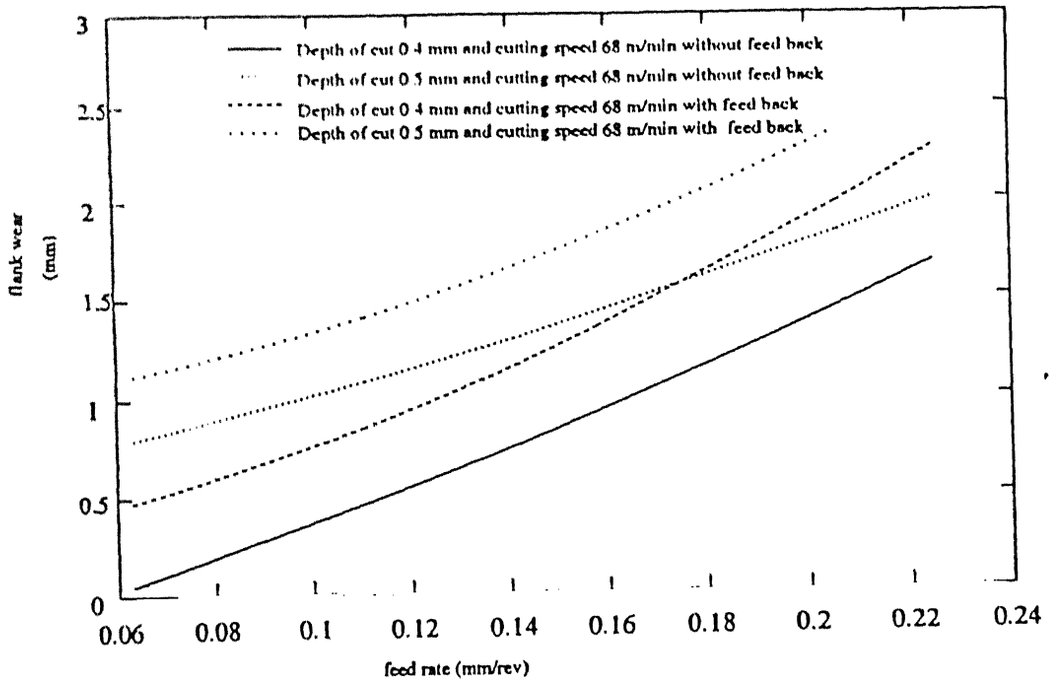

Figure 4.6: Variation of Flank wear Vs Feed rate with FB and without FB

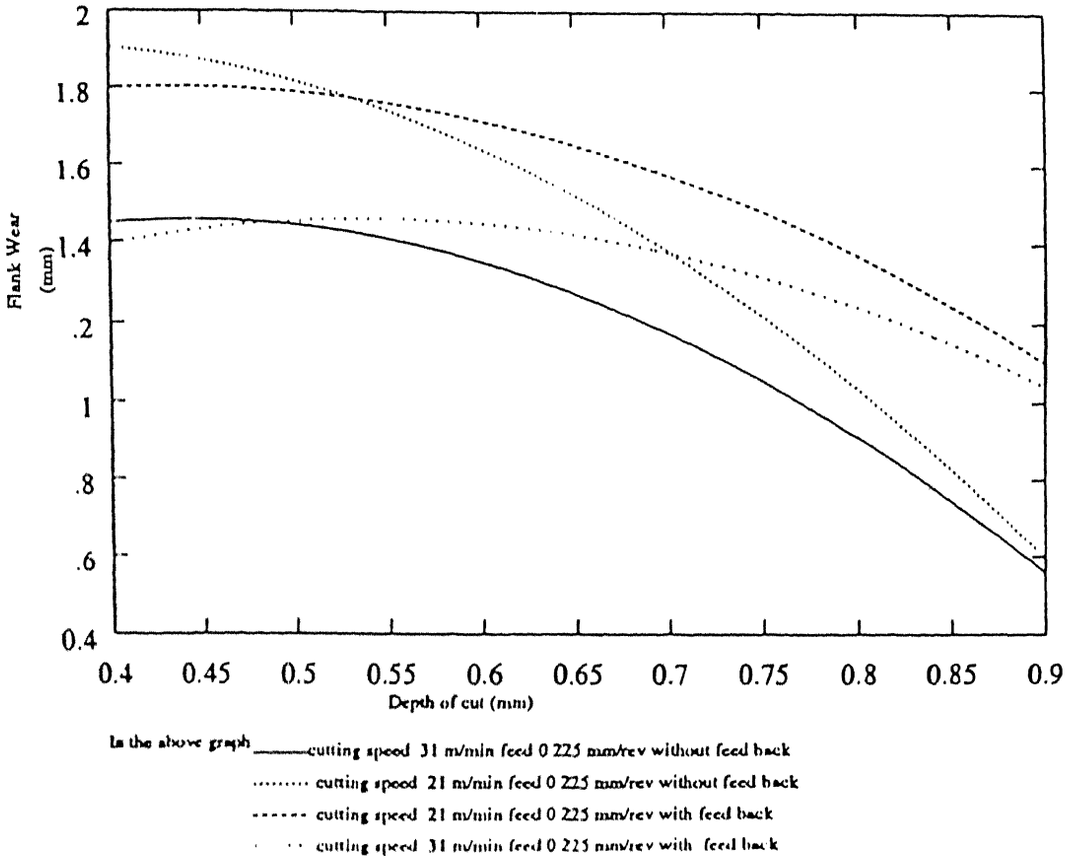

Figure 4.7: Variation of Flank wear Vs Depth of cut with FB and without FB

speeds(high temperatures). But as the cutting speed increases the hot hardness of the tool will decrease and the tool wear starts increasing. The flank wear also increases with the increase in the feed rate as shown in the Fig. 4.6. As in other cases the tool wear is also more in case of machining with the feed back system than without feed back system while varying the feed rate. The influence of the depth of cut is dependent upon the feed and speed. It varies differently with different other working conditions as shown in the figure 4.7.

The flank wear was observed to be more for machining with feed back system compared to that of machining without feed back system(as shown in the figures 4.5, 4.6 and 4.7). This is because whenever tool is moved towards workpiece to control the dimensional inaccuracy of the workpiece the tool suddenly faces the extra depth of cut and thus causes the increase in the abrasive action which results in the increase in the flank wear.

Chapter 5

Conclusions

An on-line monitoring of tool wear and control of dimensional inaccuracy using the system has been tested experimentally. From the experimental results it can be concluded that the required objectives of the present work are fulfilled. The workpiece radius change has been restricted to 0.038 mm in the worst case and 0.028 mm in the best case. The performance of the control system was tested for a range of cutting conditions. The system was found to work effectively.

The following objectives have been fulfilled.

- Design and fabrication of a sensing device to sense the tool wear during the machining.
- Design and fabrication of actuator to position the tool post according to the tool wear.
- Design of a feed back control system components like SAC(sensing and amplification circuit), PCIC(PC interfacing circuit).System was developed using the C language which is a menu driven and user friendly.

5.1 Scope for future work

The present system sensitivity can be improved still further by arranging two sensors opposite to each other one in the front slope region and another in the back slope region. The system can be used on CNC machines to develop an integrated system. The same sensing technology can be adopted for on-line measurement of out off roundness of the workpiece. The same system can be used to measure the tool wear in different machine

tools with little modifications. Presently it is developed exclusively for turning. The halogen light can also be used in place of laser light to develop a low cost system.

References

1. E.M.Trent,"Metal cutting", Butterworhts and Co.(publishers Ltd., 1984)

2. N.H.cook, "Tool wear and tool life", Journal of Engineering for Industry. vol 95, No 4, P.931(Nov,1973)

3. LiDan and J.Mathew, "Tool wear and failure monitoring techniques for turning - a review", Int. journal of machine tools and manufacture, Vol.30,No.4, p579 (1990).

4. Anuj Sanjanwala, "On-line tool wear sensing and compensation during turning operations", M.Tech thesis department of Mech.Engg.IIT kanpur 1989.

5. M.Shirasishi and K.Uehara "In-process control of workpiece dimensions in turning",Anals of CIRP,1979,vol.28/1

6. H.Suzuki and K.J.Weinmann ,"An online toolwear sensor for straight turning operations",Journal of Engineering for Industry,Trans.ASME, November 1985,Vol.107.

7. K.C.Fan and Y.H.Chao ,"In -process dimensional control of the workpiece during turning", Precision Engineering ,1991 Vol. 13, No. 1, PP. 27-32

8. M.Shirashi and S.Sato "Dimensional and Surface roughness Controls in turning Operation" Tras.ASME ,1990 80/Vol. 112 Feb

9. W.L.Jin ,P.K.Venuvinod and X.Wang "Anopotical Fiber Sensor based cutting force measuring device",International Jorunal of machine tool and Manufaturing., V0l 35, No. 6 pp 877 - 883,1995.

10. G.f.micheletti,M.koenig and H.R Victor, "Inprocess tool sensors for cutting operations",Annals of CIRP Vol 25/2/1976

11. Sqn Ldr SS Sekhon "Design of Reflective fiber-optic sensors for displacement measurements" M.Tech Thesis Feb. 1998 IIT Kanpur, India.

12. P.Cielo "Optcial techniques for industrial inspection, Academic Press Inc., Boston (1998).

13. Carl G. Looney, "Advances in feed forward neural networks: Demystifying knowledge acquiring black boxes", IEEE Transactions of Knowledge and Data Engineering, Vol.6, No.2, p211(1996)

14. W.C.Cochran and G.M.Cox,*Experimental designs*, Asia publishing House,India (1977) . Wasserman, "Neural Computing: Theory and practice", Van Nostrand Reinhold, New York, USA.

Appendix

- Workpiece material : $EN24$ steel
- Workpiece composition :
  0.35 - 0.45 % C;
  0.45 - 0.6 % Mn;
  1.3 - 1.8 % Ni;
  0.9 - 1.4 % Co;
  0.2 - 0.3 % Cr;
  0.1 - 0.35 % Si;
  rest is iron.
- Workpiece hardness : $\tilde{2}60$ BHN
- Cutting tool material : HSS with 5% Cobalt
- Cutting tool composition : 18% W, 4% Cr, 2% V, 5% Co
- Tool geometry : 0-8-4-4-12-15-0 mm
- Specification of lathe :
  Type : LB17
  center height : 170 mm
  center distance : 1000 mm
  swing over bed : 350 mm
  swing over cross slide : 170 mm
  spindle speeds : 45 - 2000 rpm
  feeds : 0.0005 - 1.4 $mm/rev.$

- Specification of A/D card : Model : PCL 812
  : 16 single analog input channels
  : 12 bit successive approximation ADC
  : switch selectable bipolar input ranges as ±1V, ± 2V, ± 5V or ± 10V
  : trigger modes by software command, programmable pacer or external pulse trigger
  : data transfer by program control, interrupt handler routine or direct memory access

- Specification of Op-amp. : Make : PMI
  Type : OP07CP
  Power supply : total voltage $\Delta V = 30$
  Maximum Voltage drift : 1.8 $\mu V/øC$
  Maximum Voltage offset : 250 μV
  Maximum curret offset : 8 nA
  Maximum current bias : 9 nA
  Pin Diagram:

- Hard Ware Control:

  Tubro c supports two hard ware control functions.

  1. inportb ( )
  2. outportb ( )